Acta Pharmaceutica Sinica B 2021;11(8):2537–2564

Chinese Pharmaceutical Association
Institute of Materia Medica, Chinese Academy of Medical Sciences

Acta Pharmaceutica Sinica B

www.elsevier.com/locate/apsb
www.sciencedirect.com

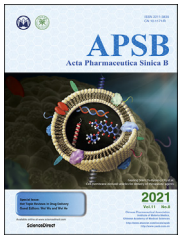

REVIEW

Pharmaceutical cocrystals: A review of preparations, physicochemical properties and applications

Minshan Guo, Xiaojie Sun, Jiahui Chen, Ting Cai*

State Key Laboratory of Natural Medicines, Department of Pharmaceutics, School of Pharmacy, China Pharmaceutical University, Nanjing 210009, China

Received 10 January 2021; received in revised form 22 February 2021; accepted 10 March 2021

KEY WORDS

Pharmaceutical cocrystals;
Cocrystal engineering;
Physicochemical properties;
Solid dosage forms;
Crystallization

Abstract Pharmaceutical cocrystals are multicomponent systems in which at least one component is an active pharmaceutical ingredient and the others are pharmaceutically acceptable ingredients. Cocrystallization of a drug substance with a coformer is a promising and emerging approach to improve the performance of pharmaceuticals, such as solubility, dissolution profile, pharmacokinetics and stability. This review article presents a comprehensive overview of pharmaceutical cocrystals, including preparation methods, physicochemical properties, and applications. Furthermore, some examples of drug cocrystals are highlighted to illustrate the effect of crystal structures on the various aspects of active pharmaceutical ingredients, such as physical stability, chemical stability, mechanical properties, optical properties, bioavailability, sustained release and therapeutic effect. This review will provide guidance for more efficient design and manufacture of pharmaceutical cocrystals with desired physicochemical properties and applications.

© 2021 Chinese Pharmaceutical Association and Institute of Materia Medica, Chinese Academy of Medical Sciences. Production and hosting by Elsevier B.V. This is an open access article under the CC BY-NC-ND license (http://creativecommons.org/licenses/by-nc-nd/4.0/).

*Corresponding author.
E-mail address: tcai@cpu.edu.cn (Ting Cai).

Peer review under responsibility of Chinese Pharmaceutical Association and Institute of Materia Medica, Chinese Academy of Medical Sciences.

https://doi.org/10.1016/j.apsb.2021.03.030

2211-3835 © 2021 Chinese Pharmaceutical Association and Institute of Materia Medica, Chinese Academy of Medical Sciences. Production and hosting by Elsevier B.V. This is an open access article under the CC BY-NC-ND license (http://creativecommons.org/licenses/by-nc-nd/4.0/).

1. Introduction

The physicochemical properties, such as the stability, particle size, powder flowability, taste, hygroscopicity, solubility and compatibility, of active pharmaceutical ingredients (APIs) are critical attributes that impact the therapeutical effectiveness and manufacturing cost of solid dosage forms[1]. In oral drug delivery systems, gastrointestinal absorption significantly depends on the solubility and dissolution rate of drug molecules. However, at present, approximately 90% of new chemical entities and 40% of currently marketed drugs belong to the Biopharmaceutical Classification System (BCS) II and IV classes, which suffer from the problems of poor water solubility and low bioavailability[2]. As a result, the absorption of drugs in the gastrointestinal tract is limited, and subsequently, the clinical applications of drugs are hindered. Obviously, the physicochemical properties of pharmaceutical solids considerably influence the performance of drug products.

It is well known that the atomic packing in the unit cell and crystal lattice directly affects the properties of a given crystalline material. Therefore, modification of the physicochemical properties of solid drug forms can be achieved by tailoring the crystal packing arrangements[3,4]. To date, several solid-state strategies have been applied to tune the properties of APIs, such as salts[5], polymorphs[6], hydrates[7], solvates[8] and cocrystals[9,10] (Fig. 1). However, these approaches have limitations; for example, only molecules with proper ionizable groups are suitable for salt formation, and hydrates/solvates are often not stable as water/solvent molecules are prone to lose over time. In comparison, any API (irrespective of acidic, basic or nonionized forms) has the opportunity to form cocrystals with a suitable coformer[3]. Over the last two decades, pharmaceutical cocrystals have attracted significant attention from academia and pharmaceutical industries due to the potential to improve the physicochemical properties of APIs by modifying the crystal structure without altering the pharmacological nature[11,12]. With the development of the cocrystal field, several pharmaceutical cocrystals have been approved, such as Steglatro®, Entresto®, and more are in clinical trials[13–16].

Pharmaceutical cocrystals are defined as crystals that comprise two or more discrete neutral molecules at a stoichiometric ratio and bond together *via* noncovalent bond interactions (*e.g.*, hydrogen bonding, van der Waals and $\pi\cdots\pi$ stacking interactions), in which at least one of the components is API and the others are pharmaceutically acceptable ingredients[17]. Since the early 2000s, it was realized that cocrystal engineering may be a potential approach to improve the physicochemical properties of pharmaceuticals, which was contributed to several representative pharmaceutical cocrystal publications in 2003−2004[9,18–20]. These pioneering works emphasized the role of crystal engineering and supramolecular synthons in pharmaceutical-based cocrystal design, which encouraged the development of the cocrystal approach to improve the drug performance. Numerous robust supramolecular synthons have been identified and shown to play important roles in cocrystal design, constituting the driving force for pharmaceutical cocrystal formation[3]. Several common functional groups are particularly amenable to the formation of supramolecular synthons of cocrystals, such as carboxylic acids, amides, and alcohols[21,22]. There are two distinct categories of supramolecular synthons, including supramolecular homosynthons and supramolecular heterosynthons[18]. Supramolecular homosynthons are formed by self-complementary functional groups, such as carboxylic acid dimers or amide dimers[23]. Conversely, supramolecular heterosynthons are organized by different but complementary functional groups (*e.g.*, the hydrogen bonding of carboxylic acid−pyridine[18] and alcohol−aromatic nitrogen[24]).

With the rapid development and increasing application of pharmaceutical cocrystals, the importance of pharmaceutical cocrystals has been concerned by regulators. In 2011, the U. S. Food and Drug Administration (FDA) first released a draft of guidance that categorized pharmaceutical cocrystals as drug product intermediates and defined them as "dissociable API-excipient molecular complexes wherein both API and excipients are present in the same crystal lattice"[14,25]. However, researchers from industry and academia considered this definition too simple to clearly differentiate cocrystals. In 2016, the revised guidelines of the FDA described cocrystals as "crystalline materials composed of two or more different molecules within the same crystal lattice associated by nonionic and noncovalent bonds"[26]. In 2018, the FDA described pharmaceutical cocrystals as "crystalline

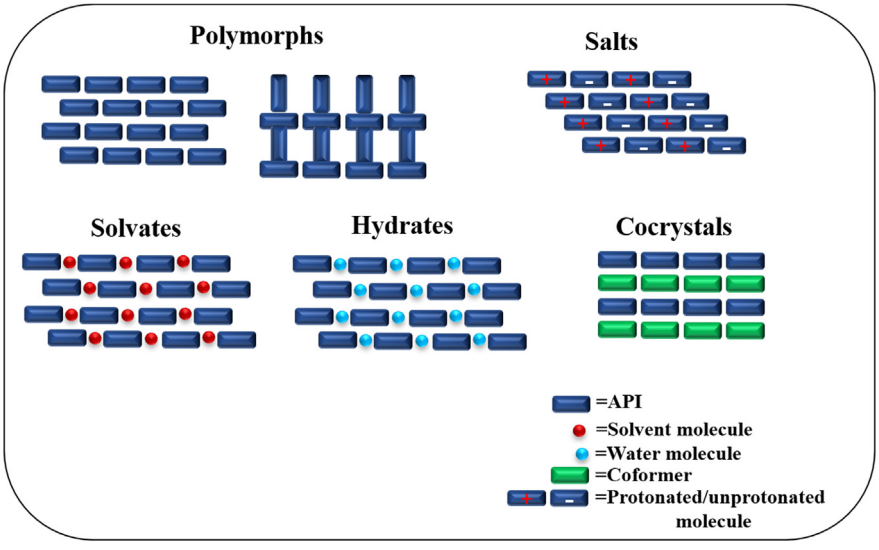

Figure 1 Different solid forms of active pharmaceutical ingredients.

materials composed of two or more different molecules, one of which is the API, in a defined stoichiometric ratio within the same crystal lattice that are associated by nonionic and noncovalent bonds". A coformer is "a component that interacts nonionically with the API in the crystal lattice, is not a solvent (including water), and is typically nonvolatile"[27]. The European Medicines Agency (EMA) defined cocrystal as "homogenous (single phase) crystalline structures made up of two or more components in a definite stoichiometric ratio where the arrangement in the crystal lattice is not based on ionic bonds (as with salts)"[28]. Compared to the definition of cocrystals by FDA, EMA described cocrystals as viable alternative to salts of the same API[28]. In other words, the cocrystal is considered the same as the API, except it shows distinct pharmacokinetic properties[29]. In this review, we will summarize the recent advances of pharmaceutical cocrystals, including preparation methods and modulations of physicochemical properties and applications of cocrystals. The solution-based method (including solvent evaporation, antisolvent method, cooling crystallization, reaction cocrystallization and slurry conversion) and the solid-based method (neat grinding, liquid-assisted grinding and melting crystallization) will be introduced. Then, the different modulated properties and applications of cocrystals will be discussed, including physical and chemical stability, mechanical and optical properties, and *in vitro* and *in vivo* performance.

2. Cocrystal preparation

To date, widespread methods have been documented for cocrystal preparation, such as solid-state grinding, solution reaction crystallization, solvent evaporation, slurry conversion and hot melt extrusion. However, the selection of a suitable cocrystallization method remains empirical. Generally, the most widely used cocrystal formation approaches can be classified as solution-based methods and solid-based methods (Fig. 2). In solution-based methods, high solvent consumption is required for dissolving the cocrystal constituents. In addition, the choice of the solvent affects the results of cocrystallization, as it can change the intermolecular interactions between API and coformer. Conversely, solid-state methods offer the potential to eliminate the requirement of solvent use in cocrystal synthesis, where no or less solvent is required.

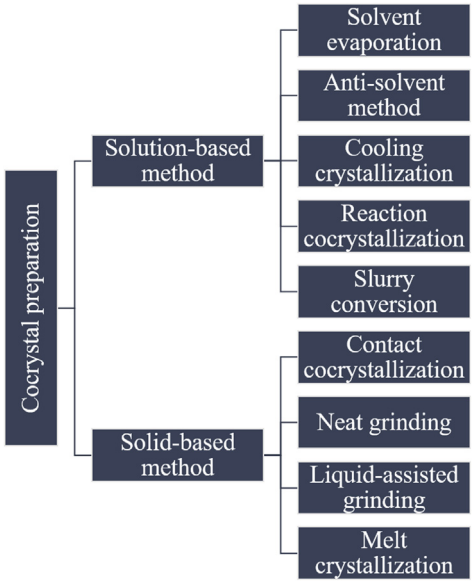

Figure 2 Common methods for cocrystal preparation.

2.1. *Solution-based methods*

In these methods, there are ternary phases (API, coformer and solvent) in the solution, and the perfect state is that the cocrystal is supersaturated while the reactants (API and coformer) are saturated or undersaturated under the experimental conditions. Hence, the degree of supersaturation with respect to cocrystal in solution is the key parameter for cocrystallization and can be adjusted by the concentrations of API and coformer[30]. To guide the path of cocrystal formation, a phase diagram that describes the conditions for thermodynamic stability must be established, which can guarantee that the cocrystal stays in the thermodynamically stable region and exclude the crystallization of pure reactants. The location of thermodynamically stable cocrystal phase regions is mainly determined by the solubility of the reactants[31]. Fig. 3 demonstrates the ternary phase diagrams, which illustrate how to reach the supersaturation of cocrystals when the reactants are in a saturated or unsaturated state, according to the solubilities of reactants[32]. As shown in Fig. 3a, reactants A and B have similar solubilities and can be congruently saturated in the given solvent; thus, cocrystals can be formed in an equivalent reactant concentration. In Fig. 3b, the reactants exhibit different solubilities in noncongruently saturating solvents, in which the cocrystal can be generated by using nonequivalent reactant concentrations to reach the cocrystal stable region.

2.1.1. *Solvent evaporation method*

Solvent evaporation is the most common method for preparing cocrystals and is typically applied for synthesizing high-quality single-crystal cocrystals that suitable for structural analysis by single-crystal X-ray diffraction. In this approach, the cocrystal constituents completely dissolve in a suitable solvent at an appropriate stoichiometric ratio and then evaporate the solvent to obtain the cocrystal[33]. The selection of solvent influences the cocrystallization, which potentially impacts the solubility of the reactants. In a given solvent, the cocrystal components should be congruently soluble. If cocrystallization process occurs between two incongruently soluble components, the less soluble component precipitates preferentially, leading to a solid mixture of cocrystal and cocrystal components, or a failure of forming cocrystals. This technique has been employed to effectively synthesize many cocrystals[33–35]. For example, a block-shaped single crystal of a 1:1 febuxostat–piroxicam cocrystal, which interacted *via* a carboxylic acid−azole synthon, was formed by slow evaporation of acetonitrile at room temperature for 3−5 days. The resulting cocrystal exhibited higher solubility and better tabletability than the corresponding components[36]. The cocrystals of nebivolol hydrochloride–nicotinamide with an improved dissolution rate were harvested by solvent evaporation[37].

2.1.2. *Antisolvent method*

Antisolvent crystallization has been considered an effective approach to control the quality, particle size and properties of cocrystals, in which crystallization is conducted in semibatch or continuous manufacturing processes[38–42]. For instance, Chun et al.[42] prepared the indomethacin−saccharin cocrystals *via* antisolvent technique. As shown in Fig. 4, a solution of 0.034 mol/L indomethacin and 0.05 mol/L saccharin was mixed in 150 mL methanol, and 75 mL water (antisolvent) was then added to the solution vessel using a peristaltic pump with a 300 rpm stirring

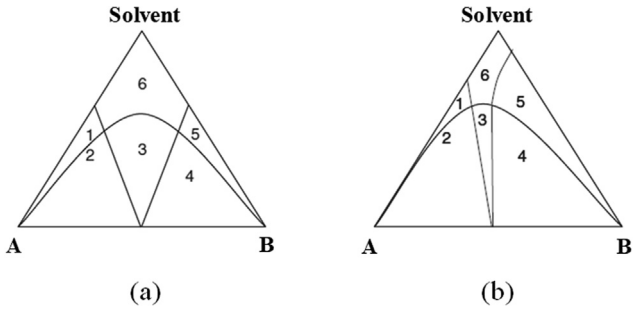

Figure 3 Isothermal ternary phase diagram of a cocrystal: (a) similar solubilities of the API and coformer in solvent; (b) different solubilities of the API and coformer in solvent; 1: A and solvent; 2: A and cocrystal; 3: cocrystal; 4: mixture of B and cocrystal; 5: B and solvent and 6: solution. Adapted from the Ref. 32 with the permission. Copyright © 2008 Royal Society of Chemistry.

speed at 25 °C for 1 h. Rod-like or columnar cocrystals with better dissolution rates were achieved. During the crystallization process, the cocrystal solubility is diminished by the addition of antisolvent to reach supersaturation, resulting in the precipitation of cocrystals. Therefore, it is critical to choose the proper miscible solvent combination in which the cocrystal has low solubility in the poor solvent. The ratio of the cosolvent can significantly influence the yield of cocrystals as the composition of the solvent could impact the solubility of the cocrystal and individual components. The yield of carbamazepine–saccharin (CBZ–SAC) cocrystals reached to the maximum value when the volume ratio of methanol to water was 1:2; whereas CBZ hydrates would form below that ratio[39]. In addition, the coformer/drug ratio was also found to be a critical attribute to cocrystal purity and solid yield. In a solution containing less SAC, CBZ hydrates tended to form as impurities during the antisolvent cocrystallization of CBZ–SAC. Since SAC exhibited a higher affinity for water than CBZ, the low content of SAC in the solution would bring more water molecules to coordinate with CBZ for forming CBZ hydrates[39].

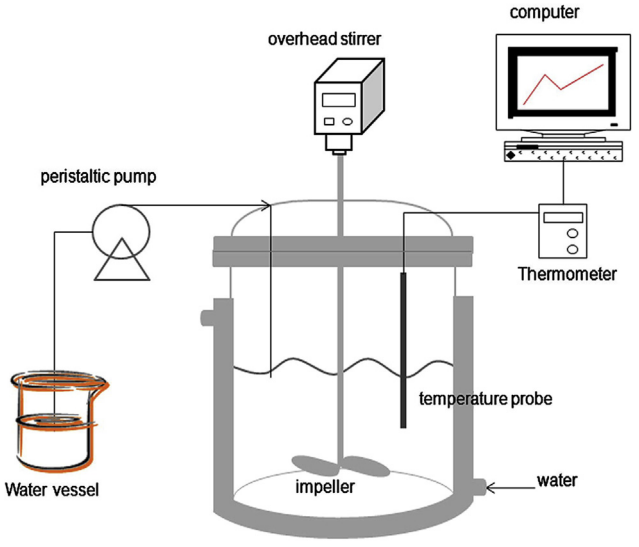

Figure 4 Experimental apparatus for the anti-solvent cocrystallization process. Adapted from the Ref. 42 with the permission Copyright © 2013 Elsevier.

2.1.3. *Cooling crystallization*

Cooling crystallization is a widely used method to prepare large-scale and purified crystals. In this method, the crystal properties of distribution size, purity, morphology and crystal polymorphism depend on the local supersaturation, which is determined by the process parameters, such as the transformation of mass and heat[43]. Hence, these factors are required to be precisely controlled according to multiple solid−liquid equilibria in the cocrystal preparation process. In the crystallization process, the operating region depends on the stoichiometry of the cocrystal, as well as the thermodynamic stability zone of the cocrystal at the start and end temperatures[44]. Several studies have shown that this method is an effective strategy for scale-up manufacturing of cocrystals[44–47]. α-Lipoic acid–nicotinamide cocrystals with kilogram yields, 99% purity, and uniform particle sizes were obtained by a continuous oscillatory baffled crystallizer (Fig. 5) at a rate of 330 g/h. To induce the nucleation of cocrystals, a 10% *w*/*w* seeding suspension was pumped into the crystallizer for 10 s at 10 °C[48].

2.1.4. *Reaction cocrystallization*

Reaction cocrystallization is suitable for cocrystal formation when the cocrystal components possess different solubilities; the reactants with nonstoichiometric concentrations are mixed to generate cocrystal supersaturated solutions, leading to cocrystal precipitation. In this method, the nucleation and growth of cocrystals are controlled by the ability of reactants to decrease the solubility of cocrystals[49]. The formation of meloxicam–salicylic cocrystals[50], carbamazepine−saccharin cocrystals[51] and indomethacin–saccharin cocrystals[52] has been achieved by reaction crystallization methods.

2.1.5. *Slurry conversion*

The slurry conversion method is a solution-mediated phase transformation process in which excess cocrystal components are required to be added to the solvent. During the slurry, each component gradually dissolves and forms a complex to promote the nucleation and growth of cocrystals. With the formation of cocrystals, the concentrations of the reactants are decreased, leading to undersaturation (with respect to the reactants) to continue to dissolve the cocrystal components. The operational range of the component's concentration and temperature is controlled by the ternary phase diagram, which guides cocrystal supersaturation generation. Huang et al.[53] found that the theophylline–benzoic acid cocrystal formation rate was significantly affected by the initial concentration of the components and the operating temperature, as evaluated by in-line Raman spectroscopy. The initial concentration of the reactants and the temperature showed a positive correlation with the cocrystal formation rate because a higher initial concentration could improve the collision probability of the components and total contact surface area; on the other hand, a higher temperature allowed the reactants to quickly reach the activated state.

2.2. *Solid-based methods*

Solid-state crystallization methods are effective and environmentally friendly in cocrystal formation as they need less or no solvent; the cocrystal forms spontaneously through direct contact or grinding with higher energy inputs. They are reasonable alternatives to solution-based cocrystallization methods, which might generate environmental hazards due to the large solvent

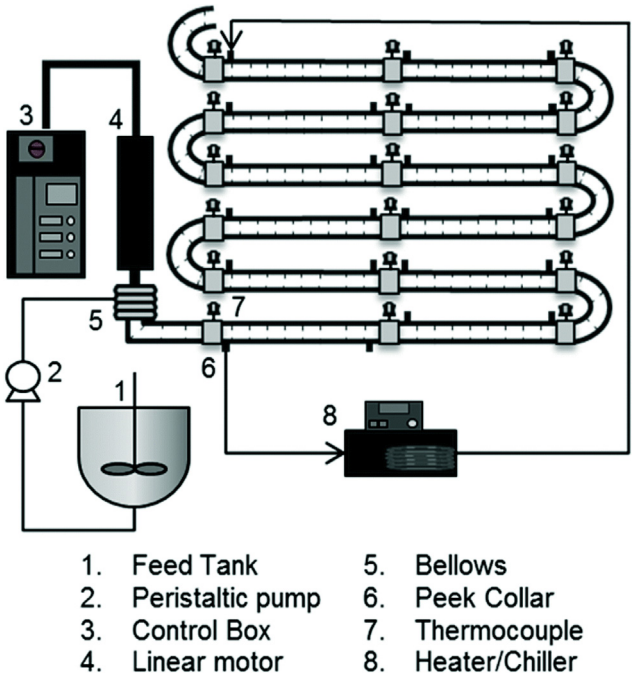

Figure 5 A schematic diagram of a continuous oscillatory baffled crystallizer (COBC). Adapted from the Ref. 48 with the permission. Copyright © 2014 Royal Society of Chemistry.

consumption. Numerous pharmaceutical cocrystals have been synthesized by solid-based methods[54–57].

2.2.1. *Contact cocrystallization*

It was found that the interactions between the API and coformer could spontaneously occur after "soft" mixing of the raw materials[58–60]. The proposed possible mechanisms explaining spontaneous crystallization by contact are vapor diffusion of the two solids, moisture sorption, eutectic phase formation, amorphization and long-range anisotropic molecular migration[61]. Higher humidity, higher temperature and smaller particle sizes of raw materials could facilitate cocrystal formation[62]. MacFhionnghaile et al.[63] described that caffeine–urea cocrystals were formed within 3 days by mixing separately premilling raw materials at room temperature and 30% relative humidity. The authors revealed that the interparticle surface contact between the solids was the key factor impacting the formation of caffeine–urea cocrystals. Ervasti et al.[64] demonstrated that the phase transformation of theophylline–nicotinamide physical mixture to cocrystal was conducted without the assistance of any mechanical grinding. Another sample of spontaneous crystallization is the cocrystallization of isoniazid and benzoic acid, which illustrated that the rearrangement of cocrystals on the isoniazid surface was accelerated in the presence of moisture by promoting the interaction of isoniazid with benzoic acid vapor[65]. Additionally, premilling of cocrystal physical mixture reduced the induction time of cocrystal nucleation and increased the cocrystal formation rate. Nartowski[66] also revealed that the kinetics of spontaneous cocrystal formation were turned by tailoring moisture addition. The deliquescence of the malonic acid surface accelerated the transition rate of caffeine–malonic acid cocrystals[66]. Ji et al.[67] demonstrated that solvent vapors could act as catalysts to accelerate the formation of caffeine–malonic acid cocrystals.

Recently, it has been reported that cocrystals could be formed by exposing cocrystal components to suitable vapors[65,68,69]. Optical microscopy studies on moisture-induced carbamazepine–nicotinamide cocrystal formation revealed that the deliquescence of components governed the cocrystal transformation, which led to localized dissolution of solid materials for crystallization[70]. Huskic et al.[71] discovered a complex and multistep dynamic pathway of cocrystal formation under methanol vapor using a benchtop powder X-ray diffractometer (Fig. 6). For carbamazepine–saccharine cocrystals, rapid formation of a short-lived crystalline phase was first observed, which then disappeared and transformed into monoclinic carbamazepine–saccharine cocrystal form II within 30 min[71]. The transformation of the carbamazepine–saccharine cocrystal form II to triclinic form I occurred after 1 h. In addition, a 1:1 nicotinamide–suberic acid intermediate was detected first and then converted to a 2:1 nicotinamide–suberic acid cocrystal, indicating that formation was dictated by competition of supramolecular synthons[71]. A similar observation was identified in the cocrystallization process of nicotinamide–fumaric acid cocrystal, in which the expected 2:1 nicotinamide–fumaric acid cocrystal was produced by a 1:1 nicotinamide–fumaric acid intermediate[71].

2.2.2. *Solid-state grinding*

The solid-state grinding method, which includes neat grinding and liquid-assisted grinding, is popular for producing cocrystals. The neat grinding method requires energy input to form the cocrystal by manual grinding (mortar and pestle) or mechanical milling (ball milling or vibratory mill) without the addition of a solvent. For liquid-assisted grinding, the cocrystal is formed by grinding with the assistance of a small amount of solvent.

2.2.3. *Neat grinding*

Previous studies have demonstrated that the potential mechanisms of cocrystal generation by neat grinding include molecular diffusion and the formation of a eutectic and or a transient amorphous intermediate[72,73]. Grinding molecular diffusion is a process in which a mobile solid surface is created by grinding, which causes vaporization or energy transfer. Hence, high vapor pressure (10^{-1} to 10^{-4} mm Hg range) of the solid-state components (at least one of the components) is essential in the neat grinding process[63]; thus, cocrystals could be formed on the crystal surface due to gas phase diffusion. Furthermore, grinding can offer energy for surface diffusion and migration to remove the generated cocrystal from the reactant surface to create a fresh surface for more cocrystallization[74]. For example, Rastogi et al.[74] found that the cocrystal formation of picric acid and aromatic hydrocarbons could be achieved by molecular diffusion with the aid of grinding. In the eutectic-induced cocrystallization process, (1) the continuous formation of an undercooled and metastable eutectic liquid phase on the fresh solid surface is indispensable and is created by agitation; (2) the nucleation of cocrystals from the eutectic phase could then be induced by grinding[72]. Chadwick et al.[72] observed a liquid eutectic phase on the interface of solids under a microscope during diphenylamine and benzophenone cocrystal formation. Furthermore, nucleation of cocrystals could lead to solidification of the liquid phase and result in the generation of cocrystals. For the amorphous-mediated cocrystallization mechanism, the strong intermolecular interactions between the API and coformer are the determining factors for cocrystal

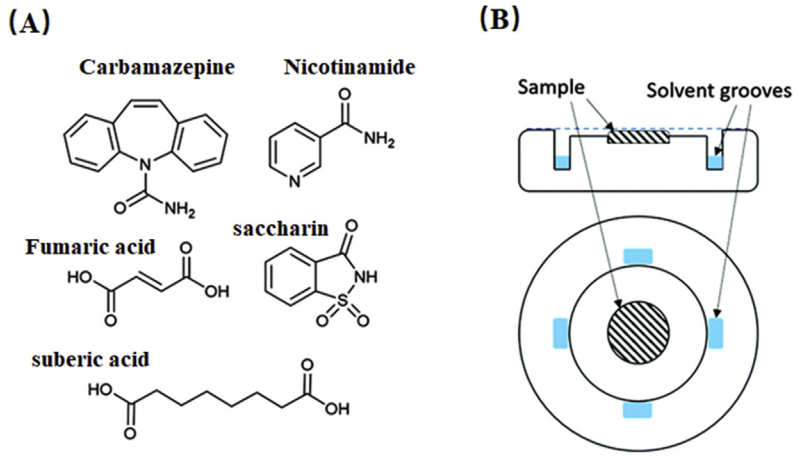

Figure 6 (A) The molecular structure of carbamazepine, nicotinamide, saccharin, fumaric and suberic acid. (B) Side-on and top views of the sample holder. Adapted from the Ref. 71 with the permission. Copyright © 2016 Royal Society of Chemistry.

formation[74]. Rodriguez-Hornedo et al.[75] observed an amorphous phase during grinding of a mixture of carbamazepine and saccharine under the glass transition temperature, and cocrystal transformation occurred during storage at room temperature. In addition, the rate of cocrystallization of carbamazepine and saccharine was enhanced by the addition of water. Rehder et al.[76] demonstrated that piroxicam–citric acid cocrystal formation is also an amorphous intermediate-induced cocrystallization process.

For neat grinding, a stepwise mechanism of cocrystal formation has been proposed, in which the kinetic and thermodynamic cocrystal product was formed[74]. This is a general feature if the reactant molecules have halogen- or hydrogen-bonding sites[77]. This mechanism is most likely due to the hierarchy of strong and weak hydrogen bonding forces during cocrystal formation. The stepwise process of 2:1 nicotinamide–suberic acid cocrystal formation *via* neat grinding was observed by Karki et al.[77] and Halasz et al.[78], wherein the 1:1 nicotinamide–suberic acid cocrystal (NA–SUB) intermediate appeared first after grinding, followed by transformation to a 2:1 nicotinamide–suberic acid cocrystal (NA_2–SUB). It was suggested that the formation of NA–SUB was kinetically driven by the strongest supramolecular synthons of amide-carboxylic acid $R_2^2(8)$ and carboxylic acid−pyridine $R_2^2(7)$ (Fig. 7). The thermodynamic product NA_2–SUB was stabilized by many slightly weaker synthons of amide−amide synthons $R_2^2(8)$ and $R_2^2(7)$ pyridine−carboxylic acid.

2.2.4. *Liquid-assisted grinding*

The liquid-assisted grinding (LAG) method is useful for generating cocrystal products with high yields and high crystallinity compared to neat grinding. In addition, this method is suitable for rapid cocrystal screening, which is independent of the solubility of the raw materials. Enhanced molecular diffusion can be achieved by the addition of a small amount of liquid, which acts as a catalyst for accelerating cocrystal formation. The selection and amount of liquid play a key role in the mechanochemical reaction, influencing the formation of different solid products and the quality of crystals. Fischer et al.[79] investigated the effect of solvent properties on 1:1 caffeine–anthranilic acid cocrystal polymorphs and found that the formation of form I appeared in the most of solvents. Form II was observed only in solvents with high dipole moments of carbonyl or nitrile groups[79]. It was explained that the precoordination of solvent molecules with the amino group of anthranilic acid led to the torsion of the caffeine at the amino-carbonyl hydrogen bond; thus, form II with a zigzag packing structure was formed rather than form I with a planar layered structure (Fig. 8)[79].The authors explained that the solvent molecules occupied many sites so that the interaction

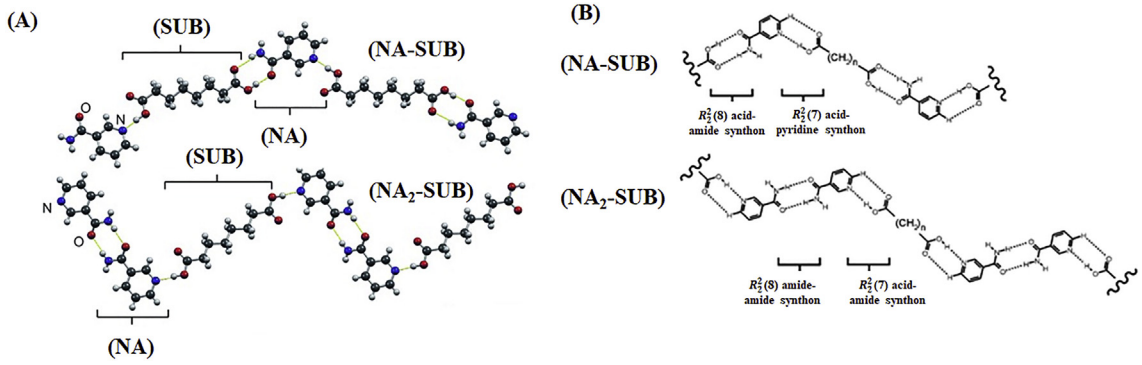

Figure 7 (A) Hydrogen-bonded chain of (NA–SUB) and (NA_2–SUB). Adapted from the Ref. 78 with the permission. Copyright © 2013 John Wiley and Sons. (B) Structure of supramolecular chains of (NA–SUB) and (NA_2–SUB). Adapted from the Ref. 77 with the permission. Copyright © 2009 Royal Society of Chemistry.

between caffeine molecules and the amino group of anthranilic acid could not take place in the same planar layer, causing caffeine twisting at approximately 30°.

Recently, Germann et al.[80] reported a hitherto unexplored effect of milling assembly on reversible mechanochemical polymorphs between stable form (form I) and metastable phases (form II) of nicotinamide–adipic acid (NIC–ADI) cocrystals during LAG, challenging the Ostwald rule of stages (Fig. 9). Both polymorphs showed zigzag structures, wherein each ADI molecule participated in the formation of two $R_2^2(7)$ or $R_2^2(8)$ synthons in form I but every ADI molecule was involved in forming both $R_2^2(7)$ and $R_2^2(8)$ motifs in form II. The corresponding relative energies of form I and form II were −7.5 and −10.2 kJ/mol, respectively. In all experiments, during the grinding process by 7 mm stainless steel ball milling with acetonitrile, the intermediate 2:1 nicotinamide–adipic acid cocrystal (NIC_2–ADI) was initially obtained. Then, metastable form II was obtained in the stainless steel jar, while thermodynamically stable form I was formed in the poly(methyl methacrylate) (PMMA) jar. In addition, form II could convert to form I by grinding in a PMMA jar, which is consistent with the Ostwald rule of stages. The opposite process was observed in the stainless steel jars, indicating the transformation of stable form I to metastable form II, in contrast to the Ostwald rule of stages. The authors speculated that this surprising phenomenon was due to the more efficient transfer of mechanical energy in the stainless steel jar (higher elastic properties) than that in the PMMA jar. Additionally, the different materials of the milling ball also significantly influence the polymorphism[80]. In the PMMA jar with stainless steel balls, transformation of the metastable form to the stable form was observed[80]. However, the conversion of form I into form II occurred in the PMMA jar when elastic zirconia (ZrO_2) balls were used to mill the raw materials[80].

Ionic liquid-assisted grinding is an emerging approach in mechanochemistry in which ionic liquids are used to replace organic solvents. In comparison with solvents, ionic liquids (ILs) have short- and long-range interactions between cations and anions, causing the properties of ILs to be controlled by modified individual or dual ionic components. The polymorphs of caffeine−citric acid cocrystal (CAF−CA) and caffeine−glutaric acid cocrystal (CAF–GLU) were successfully generated by using ionic liquids (imidazolium-based) as grinding liquids[81]. It was found that the hydrogen bonding ability of cations plays a key role in CAF−CA cocrystal form I formation rather than the polarity of the ionic liquids[81]. For the CAF–GLU cocrystal, hydrophobic and nonpolar ILs stabilized the nonpolar slip plane (200), resulting in the formation of form I[81]. The alkyl chain length of the imidazolium cation presented a negative correlation with the cocrystal formation rate. Furthermore, the change in the hydrophobic to hydrophilic properties of cations led to the alteration of form I to form II[81].

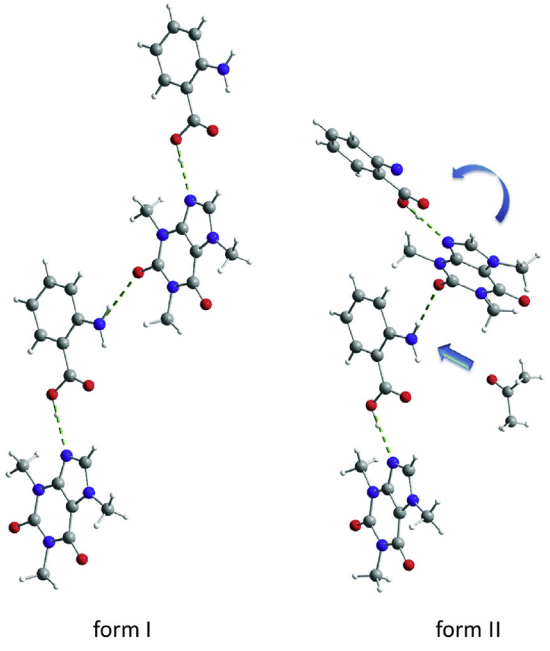

Figure 8 Crystal structure of caffeine–anthranilic acid cocrystals of form I and form II. Adapted from the Ref. 79 with the permission. Copyright © 2014 Royal Society of Chemistry.

2.2.5. *Melting crystallization*

Melting crystallization is an alternative green approach for preparing pharmaceutical cocrystals[38]. Although solvents are not involved in this approach, the thermal stability of drug and coformer should be carefully evaluated in advance[82]. Yan et al.[82] synthesized melatonin–pimelic acid cocrystal by the melt crystallization. The melatonin–pimelic acid cocrystals were formed when the molten mixture was in the temperature range of 50−70 °C. The carbamazepine–nicotinamide cocrystal was prepared by melting the physical mixture of drug and coformer at 160 °C and then cooling the melt to the ambient temperature for crystal growth[83]. Rodríguez-Hornedo and coworkers have investigated the crystallization pathways of the carbamazepine–nicotinamide cocrystal from the melt upon heating[84]. Two different pathways were found at the different heating rates: (1) at the slow heating rate (3 °C/min), a metastable phase of carbamazepine–nicotinamide cocrystal firstly nucleated and then transformed to the stable form; (2) at the fast heating rate (10 °C/min), the individual components of cocrystal crystallized first, then they were melted and the stable form of the cocrystal grew from the melt[83].

3. Physicochemical properties and applications of cocrystals

3.1. *Physical stability*

A physical change is a change in the state of a substance without any accompanying change in the chemical composition of the substance. The physical properties of solid-state materials include melting point, hygroscopicity, solubility, hardness, plasticity, elasticity, etc. Cocrystallization is a powerful approach for improving the physical properties and maintaining the physical stability of drug substances[85,86], which may suffer undesired physical transformation during manufacturing and storage. Herein, we will discuss only the melting point and hygroscopicity in this section, and other properties will be discussed in the following sections.

3.1.1. *Melting points*

For manufacturers, solid drug forms provide a convenient way to purify, identify, transport, and store drugs. For patients, solid forms are more convenient to carry and administer than liquid forms[87]. However, some drugs exist in a liquid state at room temperature due to their low melting points. Cocrystallization has the potential to alter the melting point of liquid drugs by incorporating a suitable coformer into the crystalline lattices. Propofol

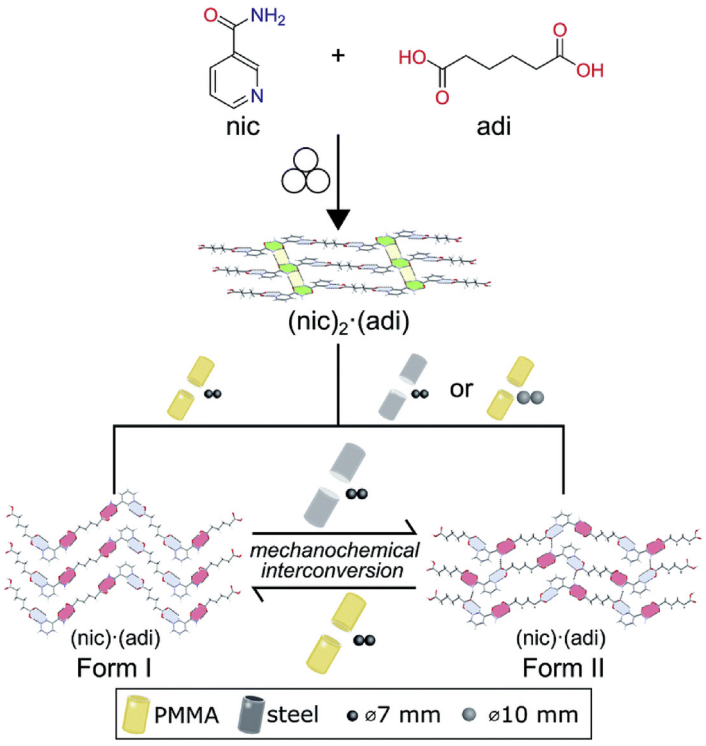

Figure 9 Schematic representation of the impact of the milling assembly, the choice and material of milling jar and balls, on the polymorphism in mechanochemical cocrystallization. Adapted from the Ref. 80 with the permission. Copyright © 2020 Royal Society of Chemistry.

is applied to induce and maintain general anesthesia and sedation. It is formulated as an oil-in-water emulsion because of its low melting point (18 °C), resulting in associated problems including instability, pain on injection and hyperlipidemia. McKellar et al.[87] adopted cocrystal approach to obtain a novel solid form of propofol using isonicotinamide as the coformer (Fig. 10). The propofol–isonicotinamide cocrystal is a stable solid at room temperature due to the increased melting point (~50 °C higher melting point than that of the starting material). Another study reported by Bacchi et al.[88] showed that cocrystals of propofol–bipyridine and propofol–phenazine could convert liquid propofol into a crystalline phase.

3.1.2. *Hygroscopicity*

The hygroscopicity of a drug substance must be thoroughly investigated because it could impact the physicochemical properties, *e.g.*, solubility, dissolution rate, stability, bioavailability and mechanical properties. For example, dasatinib anhydrate exhibited higher solubility than the monohydrate form[7,89–91]. Therefore, maintaining the hygroscopic stability of the anhydrate form is one of the major challenges during drug development. Several strategies have been applied to tackle this challenge, including adding appropriate excipients in the formulation, applying proper packing for reducing moisture uptake or coating the drug product by enteric polymers[86]. Indeed, some studies have demonstrated that cocrystal formation could improve the hygroscopic stability of drugs[86,92–94] It is suspected that the hydrogen bonds formed between API and coformer in the cocrystal could occupy the hydrogen bonding donor and acceptor sites of API to block the water molecules[95]. Huang et al.[93] demonstrated that flavonoid–theophylline cocrystals exhibited greater resistance to hydration than theophylline alone.

Caffeine is a natural alkaloid found in coffee and tea and easily forms a nonstoichiometric crystalline hydrate under humid conditions. Six cocrystals of caffeine with oxalic acid, malonic acid, maleic acid, and glutaric acid were prepared by Trask et al[96]. Among the six cocrystals, the 2:1 caffeine−oxalic acid cocrystal exhibited superior hygroscopicity stability under humidity stress for several weeks. Zileuton (ZIL) was the first drug approved for the maintenance treatment of asthma by the FDA, showing a tendency to form a stable hydrate form under moisture conditions. Cocrystals of ZIL with nicotinamide and isonicotinamide were prepared by the slurry method and demonstrated to have better hygroscopicity stability at 40 °C/75% RH for 4 weeks compared with the drug substance alone[97].

Lithium chloride (LIC), used for neuropsychiatric disorders, is extremely hygroscopic and rapidly deliquesces even at 11.30% RH, which limits its development as a drug substance. The cocrystal of LIC with glucose (GLU) showed modestly improved hygroscopic stability under 40% RH and comparable *in vivo* pharmacokinetics to those of LIC[86]. Another example of cocrystals stable to hydration is metoclopramide (MCP), a widely used antiemetic drug marketed as metoclopramide hydrochloride (MCP HCl) salt[98]. In the monohydrate form, crystallized water could trigger an ion−exchange reaction with KBr and increase the rate of the Maillard reaction with lactose during the manufacturing process[98]. The hydration of MCP HCl was effectively inhibited by using an oxalic acid cocrystal. All hydrogen bond donor and acceptor sites of MCP participated in the formation of the cocrystal, accounting for the improved stability against the moisture[98].

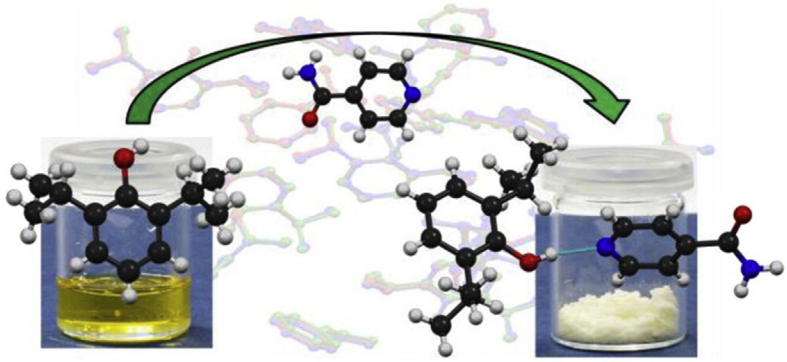

Figure 10 Conversion of liquid propofol to crystalline solid with the higher melting point by crystallizing with isonicotinamide. Adapted from the Ref. 87 with the permission. Copyright © 2014 American Chemical Society.

The nootropic drug oxiracetam (OX) is a racemic compound consisting of *S*-OX and *R*-OX. It has been reported that *S*-OX has a better therapeutic effect than *R*,*S*-OX in the treatment of cognitive dysfunction, while *S*-OX is more hygroscopic than *R*,*S*-OX. Hygroscopic tests showed that the *S*-OX–gallic acid cocrystal was less hydroscopic compared to the *S*-OX alone and the racemic parent drug, which could be attributed to the generation of complex and robust hydrogen bonded frameworks through cocrystallization[99].

3.2. *Chemical stability*

Chemical degradation of drug substances tends to occur during the manufacturing and storage stages, which challenges the development of a stable pharmaceutical formulation. It is critical to develop an effective strategy to eliminate or minimize drug degradants. Recently, pharmaceutical cocrystals have emerged as a prospective approach to overcome the chemical instability of APIs in the solid state[100,101]. Table 1 shows the list of cocrystals with enhanced photostability. Hence, this section is focused on discussing the mechanisms by which cocrystallization solves the problem of chemical degradation through changing the crystal packing of APIs. The factors giving rise to the enhancement of solid-state chemical stability by pharmaceutical cocrystals were summarized in Fig. 11. In particular, structure–property relationships were established to further provide theoretical guidance for addressing the chemical stability issues of drug candidates.

The reaction cavity refers to the space near the reaction groups in the crystal structure. A large reaction cavity causes high molecular mobility and a high probability for the occurrence of solid-state chemical reactions[102]. Epalrestat (EPR), which is used for the treatment of diabetic neuropathy, is susceptible to the photodegradation of isomerization (*E*,*Z* to *Z*,*Z*) after exposure to ambient light irradiation[103–105]. This problem not only affects the manufacturing process but also correlates to the pharmacological effect of the drug. The photostability issue of EPR was successfully addressed by crystallizing with the betaine (BET) molecule[104]. Under 6000 lx illuminance for 24 h, the color of EPR powder changed from orange to pale yellow, while surprisingly, no noticeable color change was observed for its cocrystals (Fig. 12C)[104]. It was explained that the presence of strong intermolecular interactions and a lower reaction cavity contributed to the restrained molecular motion and thus prevented isomerization (Fig. 12B and D)[104].

The distance between reactive sites plays a key role in the chemical stability of crystalline solids. For example, the drug–drug cocrystal of vitamin D3 and vitamin D2 with a greater distance between reactive sites in vitamin D resulted in improved chemical stability[106]. Nicorandil (NCD) is an effective drug for cardiovascular disorders, suffering from low chemical stability under high humidity, heat and mechanical stress (Fig. 13A)[101]. In the crystal packing of NCD, the distance between lone pair electrons on pyridines (N1) and C8 of the nearby NCD molecule is 3.367 Å (Fig. 13B), which is shorter than the sum of the van der Waals radii of C and N (3.484 Å). The close contact between N1 and C8 could facilitate the degradation process by stabilizing the carbocations ($C8^+$) of degradation intermediate Ia (Fig. 13A). Guo et al.[101] developed a series of nicorandil cocrystals with 1-hydroxy-2-naphthoic acid (1-HNA), salicylic acid (SA), 3-hydroxybenzoic acid (3-HBA), and 2,5-dihydroxybenzoic acid (2,5-DHBA). All cocrystals exhibited superior hydrothermal stability in comparison with that of NCD alone (Fig. 13C). The crystal structure of cocrystals revealed that the distances of N1–C8 were elongated and longer than the sum of the van der Waals radii of C and N (Fig. 13D). Hence, the carbocations ($C8^+$) in Ia cannot be stabilized by N1, resulting in inhibition of the catalyzed effect on the decomposition process of NCD.

Table 1 Summary of cocrystals with enhanced photostability.

API	Coformer	Ref.
Furosemide	Caffeine	
	Nicotinamide	115
Brexpiprazole	Catechol	108
Nifedipine	Isonicotinamide	116
Progesterone	Phloroglucinol	85
Antiprotozoal tinidazole	*p*-Aminobenzoic acid	117
	Salicylic acid	117
Levofloxacin	Metacetamol	95
Epalrestat	Betaine	104
Linagliptin	Ferulic acid	118
Vitamin K3	1-Hydroxy-2-naphthoic acid	114
	6-Hydroxy-2-naphthoic acid	114
	Sulfamerazine	114
Tranilast	Urea	119
	Nicotinamide	119
Nitrofurantoin	4-Hydroxybenzoic acid	120
Vitamin D3	Vitamin D2	106

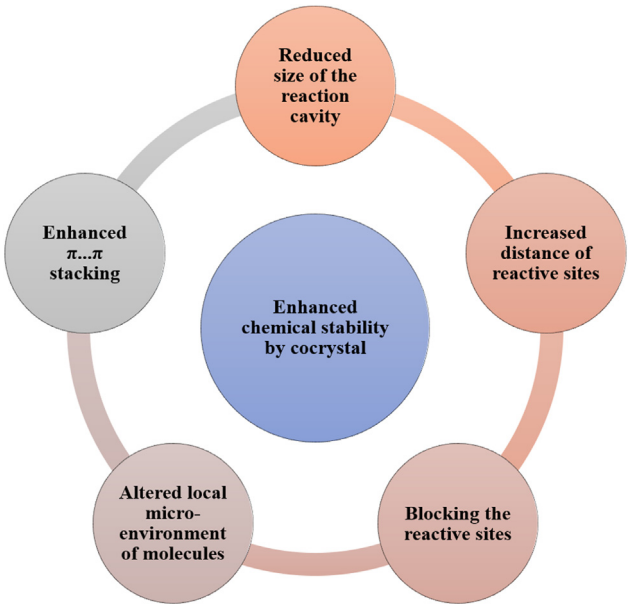

Figure 11 Diagram of the mechanisms by which cocrystals improve the chemical stability of APIs.

Brexpiprazole (BREX) has been widely applied for the treatment of atypical psychotic disorder[107,108]. It exhibits poor photostability in the presence of the polyvinyl pyrrolidone (PVP) polymer[108]. The nitrogen atom on the piperazine ring of BREX is prone to react with the peroxide in PVP and degrade into *N*-oxide impurities. The brexpiprazole−catechol cocrystal (BRC cocrystal) completely prevented the transformation of brexpiprazole to *N*-oxide degradants at 40 °C/75% for one month[108]. The improved stability of the BRC cocrystal for brexpiprazole was attributed to the strong hydrogen bonds of O−H···N (3.013(3) Å, 2.320 Å, 142.09°), which formed between the piperazine ring of BREX and the catechol molecule. The strong intermolecular interactions blocked the reactive site of the nitrogen atom on the piperazine ring, and consequently, direct contact with the peroxides was prevented[108].

Adefovir dipivoxil is an oral prodrug of adefovir with poor chemical stability[109,110]. Two degradation pathways, hydrolysis of the pivaloyloxymethyl moiety and dimerization of the adenine ring, were observed in the solid state[111,112]. Gao et al.[112] demonstrated that coformer selection for cocrystal design plays a decisive role in maintaining the solid-state hydrolytic stability of adefovir dipivoxil. Cocrystals with weakly acidic saccharin and basic nicotinamide were successfully designed and investigated. The contents of the degradation product followed the order adefovir dipivoxil–saccharin cocrystal < adefovir dipivoxil < adefovir dipivoxil–nicotinamide cocrystal after chemical stability testing for 30 days. The reason that the specific adefovir dipivoxil–saccharin cocrystal exhibited enhanced chemical stability for adefovir dipivoxil was explained by the weakly acidic nature of saccharin; thus, the adefovir dipivoxil molecule was present in a weakly acidic microenvironment, and the hydrolysis degradation of adefovir dipivoxil was inhibited. However, the nicotinamide provided a basic environment for the adefovir dipivoxil molecule, accounting for the acceleration of hydrolysis degradation.

Menadione (MD) is known as vitamin K3 and can undergo [2 + 2] photodimerization degradation in the solid state (Fig. 14A). Under sunlight, MD molecules are reoriented to an appropriate geometry for photodimerization by forming two cyclobutane photodimers[113,114]. Zhu et al.[114] prepared three MD cocrystals with 1-hydroxy-2-naphthoic acid (1-HNA), 6-hydroxy-2-naphthoic acid (6-HNA), sulfamerazine (SUL), and investigated the effect of cocrystals on the photodimerization. As expected, no obvious color change or degradation was observed for three cocrystals under 4500 lux illumination for 5 days, while a noticeable color change was observed in MD alone (Fig. 14B). It was proposed that the superior photostability of the cocrystals may result from the enhanced $\pi\cdots\pi$ stacking between MD and coformers; hence, the coformer acted as a blocker to prevent the MD molecule from approaching each other and photocyclizing[114].

3.3. *Mechanical properties*

The mechanical properties of crystalline materials are critical attributes to various manufacturing processes of solid dosage forms, such as blending, milling, granulation, tableting and coating. For solid materials, the mechanisms of mechanical deformation consist of elastic, plastic, viscoelastic, and fragmentation. Generally, materials with better plasticity properties could exhibit superior compressibility, which is permanent and irreversible after the removal of stress. However, many organic compounds have poor mechanical properties, which poses a hurdle for developing tablet formulations. Cocrystallization has been demonstrated to effectively improve the mechanical properties of drugs by altering crystal packing[121−128].

Good tableting behavior anticipates more plastic deformation and less elastic recovery for organic materials. Crystal structures with slip planes would facile plastic deformation and eventually improve the bulk compaction behavior[129,130]. Singaraju et al.[125] evaluated the compaction performance and mechanical properties of caffeine cocrystal polymorphs. The mechanical and energy framework data suggest that the better plastic deformation of caffeine–3-nitrobenzoic acid cocrystal form I (in comparison with form II) can be attributed to its 2D-layered crystal structure. For example, the powder Brillouin light scattering spectra of form I showed the presence of low-velocity shear modes, and energy framework calculations identified that a favorable slip system existed in form I[125]. Furthermore, Mishra et al.[131] investigated the mechanical properties of caffeine–glutaric acid cocrystals on different crystalline faces by nanoindentation (Fig. 15). They found that the anisotropic mechanical responses of polymorphs depended on the number of possible slip planes and the strength of the intermolecular interactions in the crystal structure with respect to the direction of indentation. The presence of higher interlayer energy, strong intermolecular interactions, and a lack of facile slip planes in form II yield hard materials (Fig. 15B and C). More facile slip planes and weaker intermolecular interactions caused form I to be soft. The results of mechanical properties indicate that form I is a potential candidate with superior tabletability compared to form II. Another example elaborated the mechanical behaviors of chlorzoxazone (a first-line therapy for muscle spasms) was reported by Roy et al[132]. Chlorzoxazone shows poor compressibility so that the wet granulation is applied to manufacture tablets. The tensile strength of tablets with chlorzoxazone alone was lower than 0.8 MPa at a compression pressure of 50 MPa. While the tensile strength of chlorzoxazone–picolinic acid cocrystals was approximately 1.6 MPa at 250 MPa without any capping or lamination. The denser packing of cocrystals (relative to pure chlorzoxazone) accounts for the enhanced bonding strength. In addition, the slip planes in the cocrystal

structure give rise to better plastic deformation of the material, resulting in the improved compressibility[132].

The punch sticking is a common problem in manufacturing tablets, where powder materials adhere to the punch surface during tableting. Based on the Paul-Sun punch sticking model, F1 (API-punch adhesion), F2 (API−API cohesion) and F3 (API-excipient adhesion) play a key role in the punch sticking propensity[133]. There are three situations according to the values of F1, F2 and F3: (1) if F1 is higher than F2 and F3, API sticking will occur; (2) if F2 < F3, only a monolayer of API will form on the punch; and (3) if F2 > F3, the layer coated on the punch tips will continuously build up[134]. APIs with high plasticity exhibit serious punch sticking issues due to their increased contact area of API-punch and API−API and thereby enhance the values of F1 and F2. Sun and coworkers[134] speculated that this problem could be minimized or even eliminated by using a harder crystal form. Celecoxib (CEL) is a nonsteroidal anti-inflammatory drug for the treatment of arthritis, acute pain, and menstrual pain. The CEL exhibits a serious punch sticking propensity due to the presence of slip planes in the crystal structure. The cocrystal of celecoxib–L-proline (CEL–PRO) shows a lower punch sticking propensity than the pure CEL due to the formation of strong interlayer bonding energy, deactivating slip planes and weaker API−API interactions (F2) in the structure of the cocrystal (Fig. 16B and C)[134]. Furthermore, according to the results of the molecular electrostatic potential maps, the electronegativity of the exposed portion on the pyrrolidine group in L-proline is lower than that of the carbon−fluorine functional group of CEL, resulting in the exposure of electronegative groups on the punch tips decreasing and hence lowering the initiation of sticking (reduced F1)[134]. Therefore, celecoxib–L-proline cocrystals are more suitable for tableting than the pure CEL crystals.

Organic crystals are usually brittle and fragile, which largely limit their applications in the fields of pharmaceuticals[135], biomaterials[136], optoelectronics[137], fluorescence[138] and semiconductors[139]. Recently, some studies have reported that a few organic materials could achieve high flexibility by cocrystallization with a suitable coformer[140,141]. Ghosh et al.[140] reported a remarkably elastic and bendable cocrystal of caffeine–4-chloro-3-nitrobenzoic acid methanol solvate, which displayed reversible blending after withdrawing the mechanical force (Fig. 17A). The high flexibility and excellent shape recovery could be ascribed to structural characteristics such as an interlocked host structure without slip planes, weaker and dispersive interactions in the crystal, and mobile methanol solvent channels (Fig. 17B). Furthermore, Mei and coworkers[142] reported a 2:1 cocrystal of vitamin D and cholesterol with spring-like hydrogen bond networks, which formed through self-assembly of e−OH− and a−OH−substituted cyclohexanol derivatives. In this system, the supramolecular interacting helix could sustain macroscopic flexibility throughout amplifying the elastic "spring" from many length scales. When impacting three-point local pressure on the (100) face, reversible bending occurred due to the region of "structural buffering" of the soft alkyl chains and exhibited a spring-like skeleton accompanied by looser packing (d = 2.10 Å) along the direction of hydrogen bond interactions. Hence, this face could accommodate specific stress without the occurrence of permanent slippage of molecules. Simultaneously, irreversible deformation on the (001) planes was observed because layers glide each other and without any alternation of

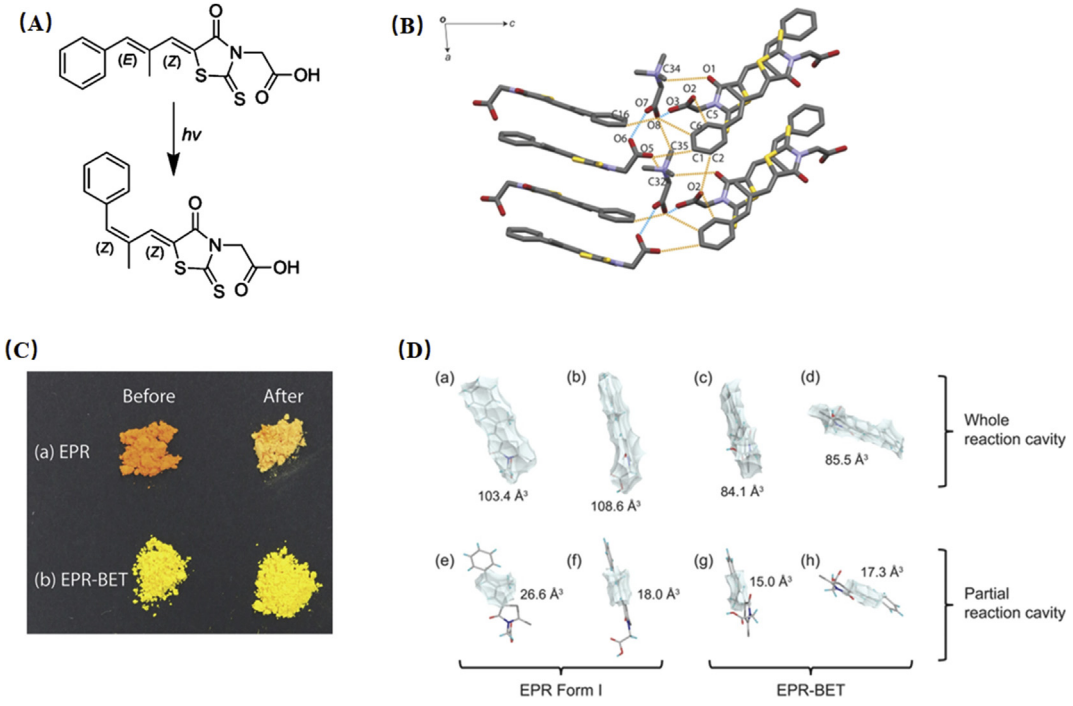

Figure 12 (A) Chemical structure and photoisomerization of EPR upon exposure to light. (B) The hydrogen bond architectures of EPR–BET cocrystal. (C) The color change of EPR and EPR–BET cocrystal before and after irradiation. (D) Whole and partial reaction cavity of EPR form I (a, b, e, f) and EPR–BET cocrystals (c, d, g, h). Adapted from the Ref. 104 with the permission. Copyright © 2018 American Chemical Society.

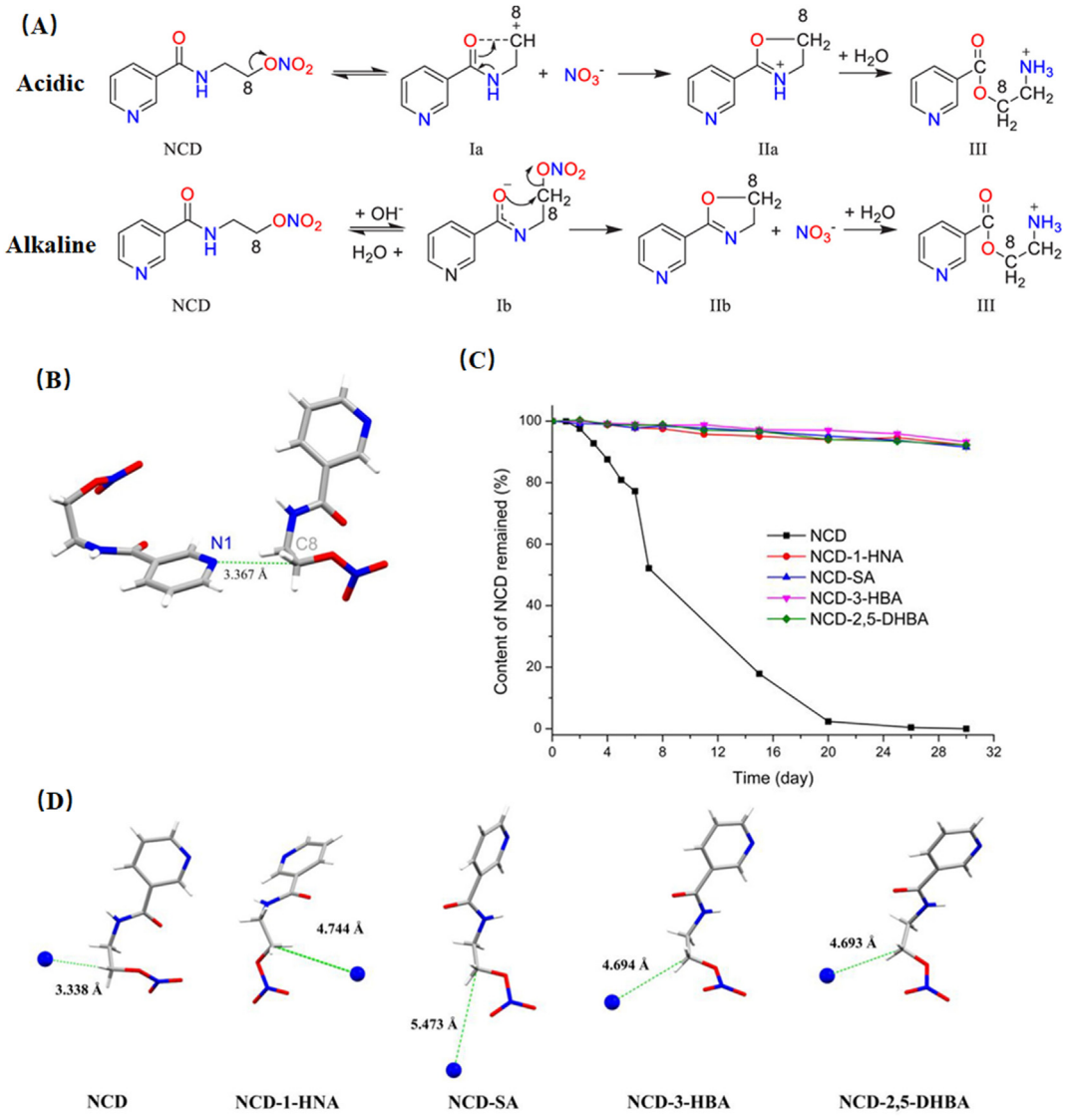

Figure 13 (A) Degradation mechanism of NCD in different environments: acidic and alkaline. (B) Distance between the nitrogen atom (N1) of the pyridine ring and the carbon atom (C8) of the ethyl group in the crystal structure of NCD (CCDC 1161948). (C) The content of NCD remained after hydrothermal stability testing. (D) Summary and comparison of the shortest distances between N1 and C8 in NCD and each cocrystal. Adapted from the Ref. 101 with the permission. Copyright © 2020 American Chemical Society.

distances of molecules when local stress was applied in the cocrystal.

3.4. *Optical properties*

The optical properties of drugs could be useful in biomedical applications. For example, drugs that exhibit strong fluorescence can be used as biocompatible probes for bioimaging[143] and lipid droplet imaging in cells and in tissue slices[144].The molecular stacking, crystal packing arrangement and intermolecular interactions usually play important roles in the optical properties of solid materials[145–147]. Recently, cocrystal engineering has shown its potential to modify the optical properties of pharmaceuticals[53,148,149]. The following examples shows the modification of the optical behavior of drugs by introducing coformers into the crystal lattices.

The colorless furosemide (FS) is a BCS IV drug for the treatment of edema and hypertension. The polymorphic cocrystals of FS and 4,4′-bipyridine (4BPY, colorless) were pale yellow and orange for form I and form II, respectively (Fig. 18A and B)[150]. Both polymorphs have a similar sandwich centrosymmetric structure, formed by aromatic $\pi\cdots\pi$ stacking interactions in the form of an "FS-4BPY-FS" arrangement (Fig. 18C). In form I, the sandwich motif comprises the C—H$\cdots\pi$ interactions between the H atom of 4BPY and the π electrons of the furan, as well as the $\pi\cdots\pi$ interactions between FS and 4BPY. In form II, $\pi\cdots\pi$ interactions and C=O$\cdots\pi$ interactions are engaged in the sandwich assembly. The authors proposed that the different π-stacking patterns and hydrogen bonding interactions in the polymorphs lead to differences in color. The HOMO (highest occupied molecular orbital) and LUMO (lowest unoccupied molecular orbital) gaps of cocrystals were further calculated by the DFT (density functional theory) simulation, which revealed that the band

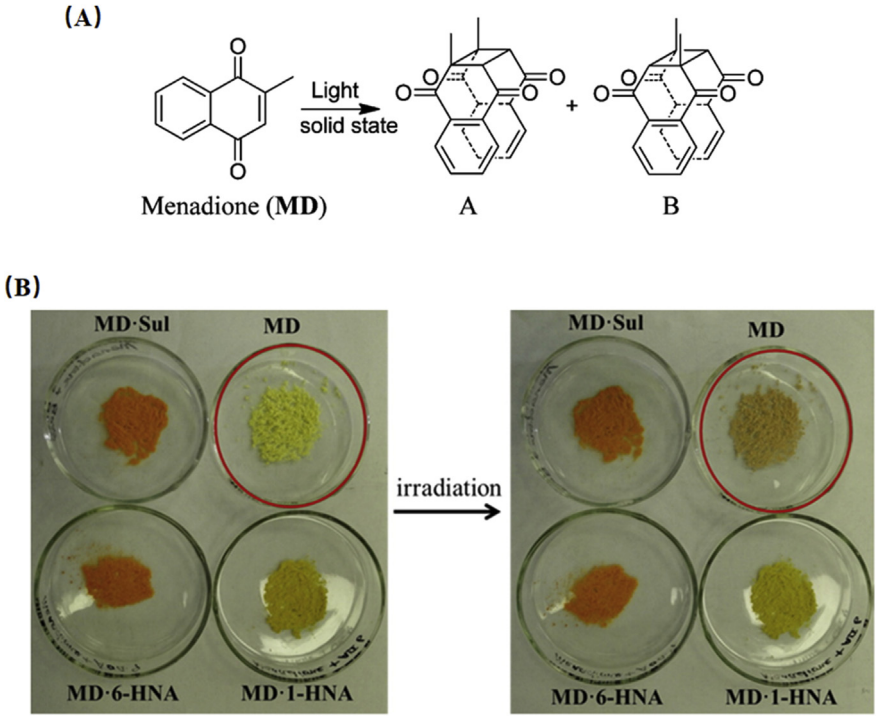

Figure 14 (A) Chemical structures of MD and its photoproducts. (B) Change in physical appearance of MD and its three cocrystals with an illumination of 4500 lux for 5 days. Adapted from the Ref. 114 with the permission. Copyright © 2016 American Chemical Society.

gap of form II was lower than that of form I, accounting for the different colors of two polymorphs[150].

Emodin (EM) is a natural pigment with several pharmacological activities, such as anti-inflammatory, cathartic, anticancer and antioxidative activities. The color of EM was tuned from yellow to dark red by cocrystallization with a series of colorless coformers[149]. Li et al.[149] argued that $\pi\cdots\pi$ and charge-transfer interactions contribute to the color transit from yellow to red.

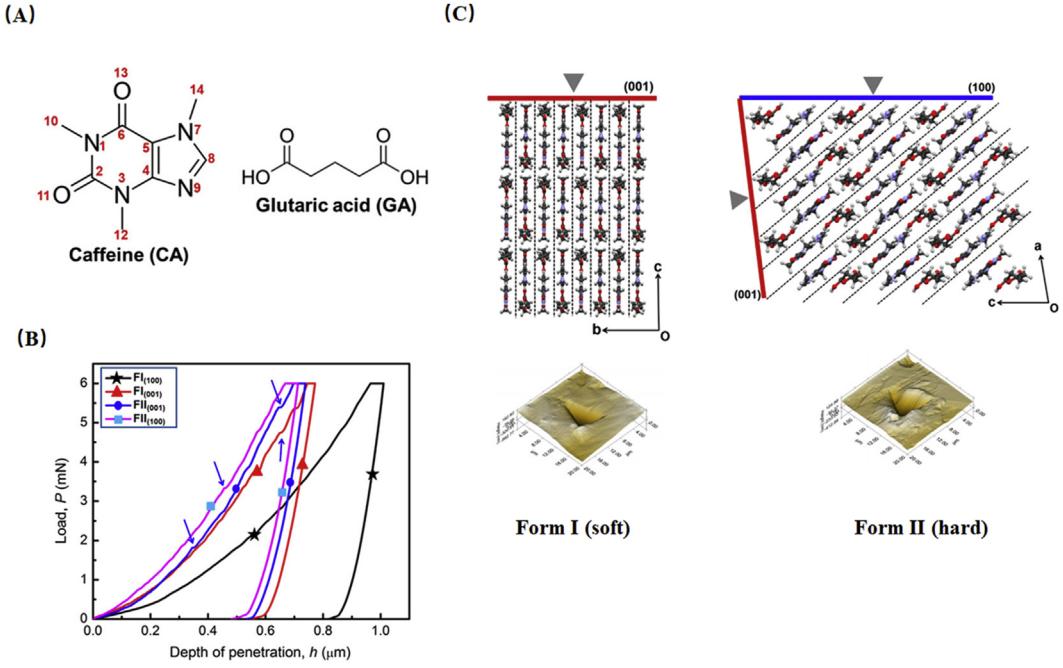

Figure 15 (A) The chemical structure of caffeine and glutaric acid. (B) Representative *P*–*h* curves of the caffeine–glutaric acid cocrystal. Blue arrows represent pop-in. (C) Crystal structure of form I and form II and a pictorial representation of softness−hardness modulation. Adapted from the Ref. 131 with the permission. Copyright © 2020 American Chemical Society.

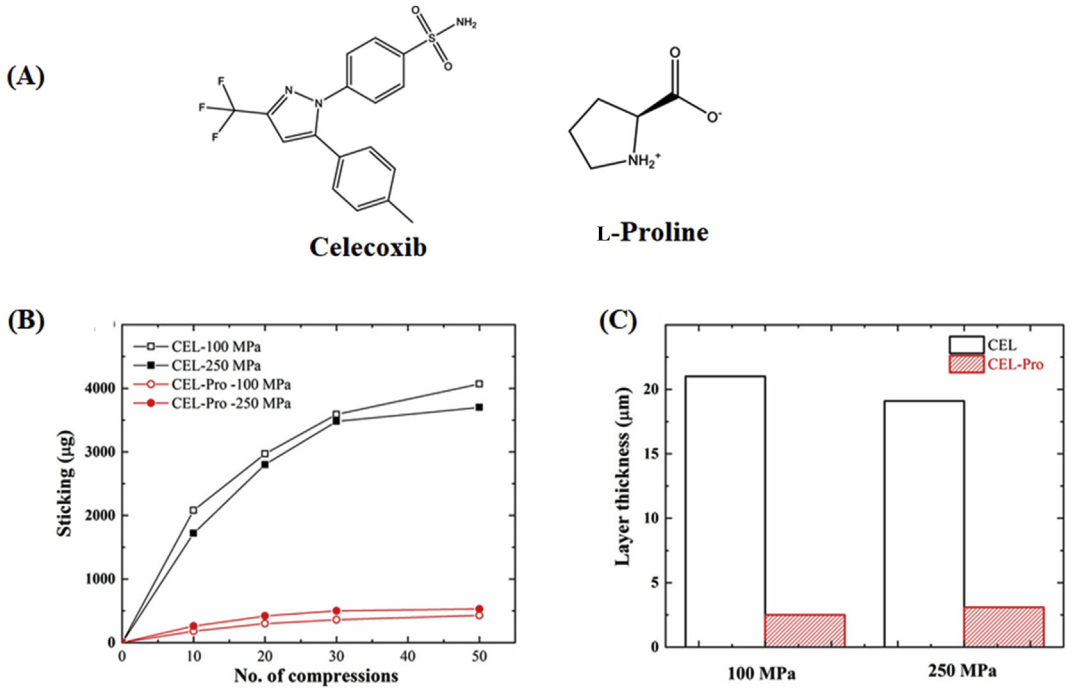

Figure 16 (A) Chemical structure of celecoxib and L-proline. (B) Sticking propensity and (C) sticking layer thickness of celecoxib form III and celecoxib–L-proline cocrystal formulations (20% active in the MCC matrix) at compaction pressures of 100 and 250 MPa. Adapted from the Ref. 134 with the permission. Copyright © 2020 American Chemical Society.

The stronger $\pi\cdots\pi$ interactions could promote the charge-transfer process from the excited state to the ground state, leading to a redshift in the maximum absorption wavelength.

Phloretin (PHL), a natural phenol, has attracted attention from researchers due to its antioxidative and anti-inflammatory effects. Cocrystals of PHL with nicotinamide (NIC) and isonicotinamide (INM) exhibit different emission properties[17]. Under 365 nm ultraviolet (UV) irradiation, the phloretin–nicotinamide (PHL–NIC) cocrystal shows the strong yellowish-green fluorescence, while no fluorescence of the phloretin–isonicotinamide cocrystal (PHL–INM cocrystal) is observed (Fig. 19). The distinct photoluminescent properties between PHL–NIC cocrystal and PHL–INM cocrystal could be attributed to the different packing arrangement and intermolecular interactions of PHL and coformers[17].

3.5. *Bioavailability*

Bioavailability refers to the fraction of the drug that reaches systemic circulation. Numerous drug candidates failed in the preclinical stage during drug development because of the low bioavailability. In the last decade, cocrystallization has shown its potential to improve *in vivo* performance by enhancing the solubility, and bioavailability of poorly water-soluble drugs[151–155].

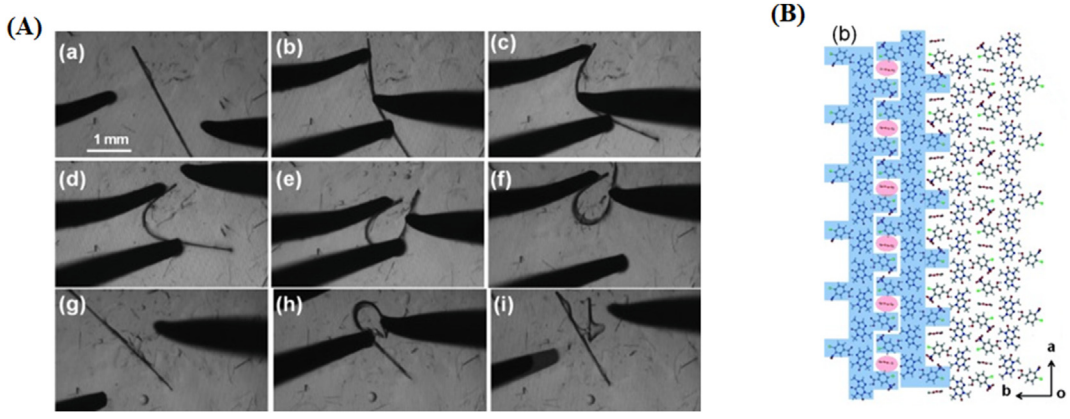

Figure 17 (A) Image of elastic bending of cocrystal solvate: (a–f) first bending cycle by a pair of forceps and a metal pin; (g) crystal shape recovery after withdrawing the mechanical force; (h) second bending cycle; (i) the breaking of crystal when applied stress exceeded the elastic limit. (B) Interlocked structure (blue) and mobile methanol solvent channels (red). Adapted from the Ref. 140 with the permission. Copyright © 2012 John Wiley and Sons.

This strategy is especially suitable for drugs unable to form salts due to the lack of ionizable functional groups.

Ketoconazole, a broad-spectrum imidazole antifungal agent, exhibits low bioavailability because of its very low water solubility. The cocrystal of ketoconazole–*p*-aminobenzoic acid showed 10-fold higher aqueous solubility and 6.7-fold higher oral bioavailability than crystalline ketoconazole[156]. Apigenin (APG) is a bioflavonoid with many pharmacological activities, such as anti-inflammatory, anticarcinogenic and antibiotic properties[157]. However, the clinical application of APG is limited due to its extremely low solubility and bioavailability. The cocrystal of APG and 4,4′-bipyridine yielded 3.9-fold higher bioavailability than the parent drug[157]. Another sample, ambrisentan (AMT), is an endothelin type A receptor blocker and is approved for the treatment of pulmonary arterial hypertension[158]. The poor water solubility (0.06 mg/mL) of AMT categorizes it as a compound of BCS class II[158]. The cocrystal of AMT with glycylglycine (GG) is constructed by the supramolecular synthon networks, the carbonyl in AMT interact with OH_{acid} groups of GG ($C{=}O\cdots OH_{acid}$) as well as OH_{acid} of another AMT molecule, leading to the bifurcated $C{=}O\cdots HO_{acid}$ interactions. The cocrystal of AMT-GG shows 2.7-fold enhancement of C_{max} (maximum plasma concentration) and nearly 2-fold increase in the value of AUC (area under plasma concentrations−time curve) in comparison with pure AMT[158]. Baicalein is a well-known flavonoid with various pharmacological activities, such as antibacterial, anti-inflammatory, antiadipogenic, anticancer, and anti-HIV activities[154]. Unfortunately, the bioavailability of baicalein is quite low largely due to its poor water solubility (16 μg/mL). Cocrystal of baicalein with caffeine exhibited the superior pharmacokinetic property, the relative bioavailability of the cocrystal was enhanced by 4-fold in comparison with neat baicalein or physical mixtures on the basis of AUC0–24 h[154].

The solution-mediated phase transformation may occur during the dissolution process of highly soluble cocrystals, in which the poorly soluble drugs precipitate out of solutions, diminishing the solubility advantage of cocrystals. This problem means that cocrystallization does not always have the positive effect on the solubility and bioavailability of the drugs. Thus, delaying or eliminating the process of solution-mediated phase transformation is essential to prolong the supersaturation for enhancing the bioavailability of poorly water-soluble drugs[151,159]. Childs et al.[151] reported that the cocrystal of danazol−vanillin yielded only a 1.7 times higher AUC than the parent drug. However, over 10-fold improvement in oral bioavailability was achieved for the cocrystal dissolved in the presence of a solubilizing agent (1% vitamin E-TPGS) and a crystallization inhibitor (2% Klucel), where the supersaturation was maintained. Carbamazepine–succinic acid cocrystals underwent rapid phase transformation to the low-soluble parent drug during the dissolution process[160]. The bioavailability of carbamazepine–succinic acid cocrystals was improved by impeding the precipitation of carbamazepine using 1% hydroxypropylmethylcellulose acetate succinate (HPMCAS) and 2% polyvinyl caprolactam-polyvinyl acetate polyethylene glycol graft copolymer® as crystallization inhibitors. Approximately 6-fold enhancement in AUC and 4-fold enhancement in C_{max} were achieved in comparison with the unformulated "neat" cocrystal. In addition, surfactants may have significant impacts on maintaining the supersaturation created by dissolution of cocrystals[161]. Alhalaweh et al.[161] studied the effect of the surfactant (sodium lauryl sulfate) on the dissolution of carbamazepine–saccharin cocrystal and found that the surfactant could act as a

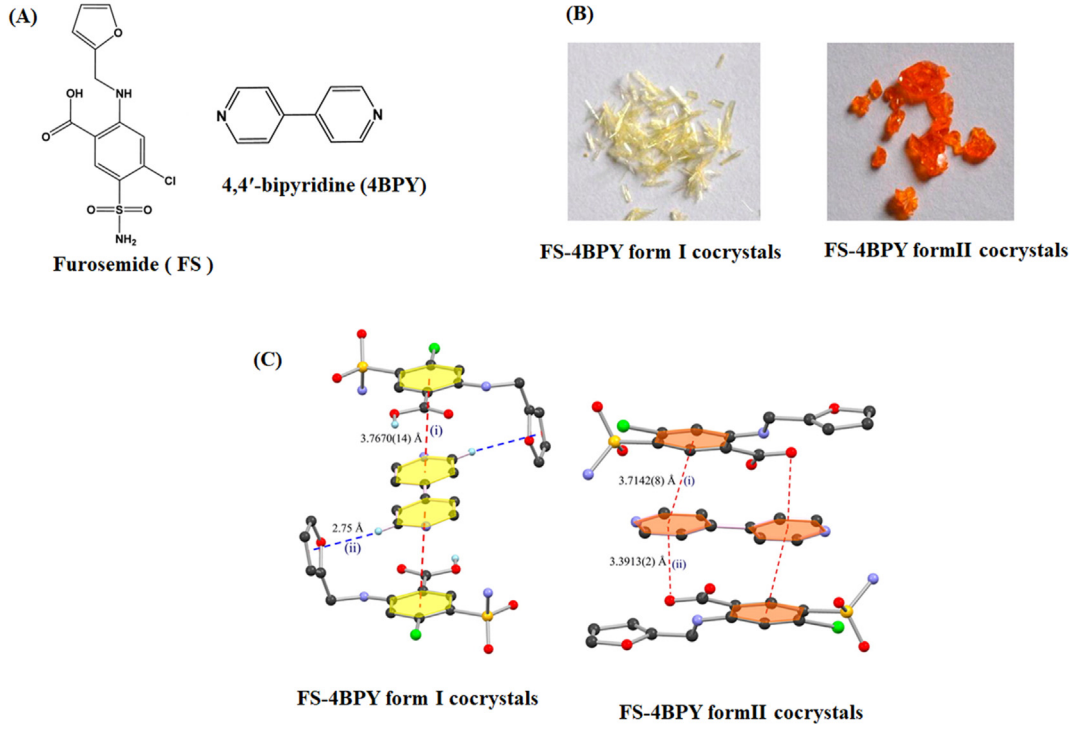

Figure 18 (A) Molecular structure of furosemide and 4,4′-bipyridine. (B) Photographs of FS–4BPY cocrystals from I and form II. (C) Crystal structure of FS–4BPY cocrystals from I and form II. Adapted from the Ref. 150 with the permission. Copyright © 2015 American Chemical Society.

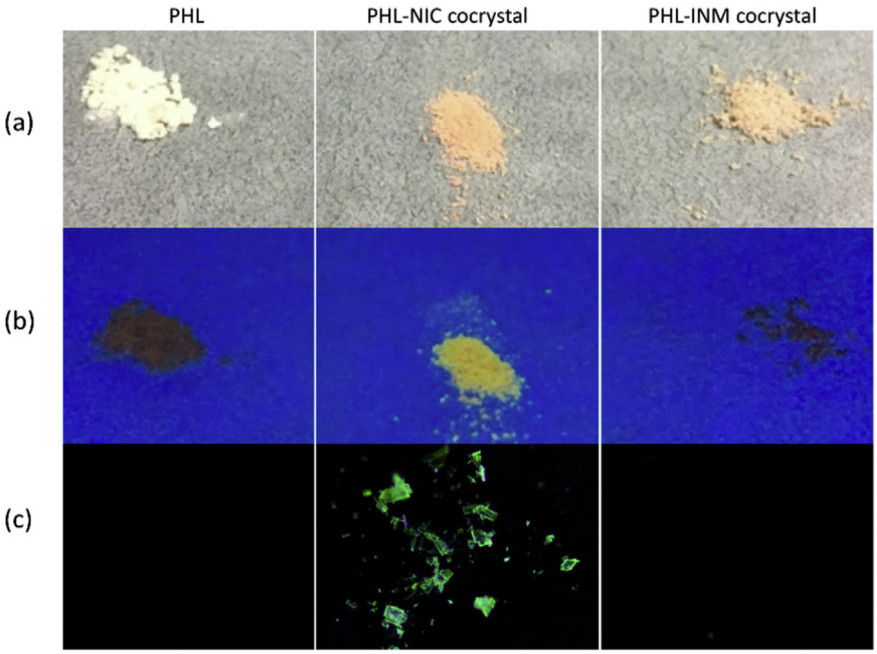

Figure 19 Photographs of solid-state cocrystal samples (from left to right: PHL, PHL–NIC cocrystal and PHL–INM cocrystal): (a) the powder samples under daylight; (b) the powder samples under UV (365 nm) lamp; (c) the single crystal samples under UV (365 nm) observed by polarized microscope. Adapted from the Ref. 17 with the permission. Copyright © 2019 American Chemical Society.

solubilizing agent to increase the solubility of the drug, which turned out to prolong the supersaturation by reducing the driving force of crystallization. Rodríguez-Hornedo and coworkers[161] also demonstrated that the surfactant could decrease the solubility advantage ($solubility_{cocrystal}/solubility_{drug}$) of indomethacin–saccharin cocrystal and sequentially sustain the supersaturation. The increased solubility of the drug in the presence of surfactant lowered the driving force of nucleation, and thus the recrystallization was less favorable.

3.6. *Sustained release*

The sustained release dosage form exhibits considerable advantages in reduced dosing frequency, improved patient compliance, and mitigated side effects due to the steady-state blood level with less plasma fluctuations. Various formulation strategies have been used to achieve sustained release profiles, such as polymeric matrices[162], membrane-controlled[163] and osmotic pump drug delivery systems[164]. In the recent years, cocrystallization has been demonstrated as an alternative approach to sustain the drug release[165–170]. For example, the half-life of nicorandil (NCD) was prolonged by cocrystallizing with poorly soluble organic acids, such as 1-hydroxy-2-naphthoic acid (1-HNA) and salicylic acid (SA)[101]. The NCD–1-HNA cocrystal displayed a reduction in the dissolution rate by approximately 22.7, 21.6 and 7.4 times in pH 2.0, 4.6, and 6.8 buffer, respectively, compared with pure NCD. The cocrystal of zonisamide with caffeine and L-proline exhibited a lower solubility and dissolution rate than pure zonisamide, indicating the potential for developing sustained-release formulations of zonisamide to solve the problem of half-life fluctuations[166]. In addition, the sulfonamide class drugs sulfamethazole[171,172] and sulfacetamide[172] have unsatisfactory bioavailability due to their short *in vivo* elimination half-lives. For the drugs with fast systemic elimination, forming the cocrystals with lower equilibrium solubility and intrinsic dissolution rates could potentially serve as the approach to release the drugs sustainedly, resulting in the enhanced bioavailability[171,172].

Isoniazid (INH) is one of the first-line drugs for tuberculosis, which requires a large dose for long-term treatment, resulting in poor patient compliance, severe side effects of hepatotoxicity and drug resistance. Xuan et al.[173] successfully developed an extended release form of isoniazid by cocrystallizing it with a hydrophobic coformer (curcumin). It has been reported that the thermodynamic solubility of cocrystals is related to the solubility of coformers, in which a lower soluble coformer could produce a cocrystal with low water solubility[174]. Hence, the isoniazid–curcumin cocrystal has the low solubility by incorporating the poor soluble curcumin molecule into the same crystalline lattice. At pH 1.2, INH was completely released from the physical mixture after 15 min (Fig. 20B). However, only 28% of INH was dissolved from the cocrystal after 15 min, followed by sustained release, in which 73% of INH was released after 48 h (Fig. 20B and C). The authors attributed the reduced dissolution rate of the INH cocrystal to two reasons: (1) the introduction of low water-soluble curcumin (CUR) into the INH crystal lattice would block the solvation sites of IHN, thereby reducing its release rate; (2) CUR form III precipitated out of solution and covered at the cocrystal surface to inhibit the dissolution of INH from cocrystals. In contrast, INH was completely released after 24 h in pH 6.8 solution (Fig. 20C). The distinct release behaviors between different pH values are due to the different recrystallization kinetics of CUR.

Yu et al.[158]studied the factor of cocrystal structure on influencing the release profiles of piperazine ferulate salt (PRZ–FLA), which has been used for treating kidney diseases. However, the short plasma half-life of PRZ–FLA render it difficult to achieve therapeutic plasma levels by the oral administration[158]. A ternary cocrystal (piperazine–ferulate–pyrazinamide, PRZ–FLA–PRA) was designed to achieve the sustained release of drugs[158]. In the structure of PRZ–FLA–PRA cocrystal, the PRZ–FLA connected

with PRA dimers by the strong hydrogen bonding interactions to form a tight network (Fig. 21B). The hydrophilicity of PRZ–FLA was significantly decreased after forming the cocrystal since the solvation sites of PRZ–FLA was reduced from the structural perspective. The solubility of PRZ–FLA from cocrystals were lower than those of pure PRZ–FLA in different dissolution media at pH 1.2, 4.0 and 6.8 (Fig. 21C). As expected, the intrinsic dissolution rate of the PRZ–FLA salt decreased upon forming the ternary PRZ–FLA–PRA cocrystal (Fig. 21D).

The solubility APIs are correlated with lattice stabilities and intermolecular interactions in crystals[175]. Kumari et al.[175] demonstrated that the solubility and dissolution rate of pirfenidone (PFD) would be decreased by cocrystallizing with a suitable coformer to increase the crystal lattice and intermolecular interaction energy (Fig. 22). PFD is a new drug molecule used for healing idiopathic lung fibrosis (approved by the FDA in 2014)[175]. The high-dose pirfenidone shows serious side effects[175]. The cocrystals of pirfenidone–fumaric acid (PFD–FA) and pirfenidone–trimesic acid (PFD–TA) yielded 50% and 90% reduced solubility of PFD, respectively. The solubility of PFD followed the order PFD > PFD–FA cocrystal > PFD–TA cocrystal, which was consistent with the observation that $E_{lattice}$ (PFD–FA cocrystal) > $E_{lattice}$ (PFD) as well as that E_{bind} (PFD–TA cocrystal) > E_{bind} (PFD–FA cocrystal). The authors proposed that the strong intermolecular force of cocrystals yielded high heat of fusion and hence reduced cocrystal solubility[175].

3.7. *Therapeutic effect*

The therapeutic effect of a drug substance is often influenced by its physicochemical properties. The limitation of low solubility or permeability of BSC II and BCS IV class drugs would immensely restrict the therapeutic effect of the medicines. The cocrystal strategy has been considered an effective technique to improve bioavailability and thus enhance the therapeutic effect[176–178]. Table 2 shows a summary of reported cocrystals with enhanced therapeutic effects. Yu et al.[179] studied the anticancer activities of tegafur after forming the cocrystal with a nutraceutical component, syringic acid (Fig. 23). *In vitro* cytotoxicity testing showed that tegafur–syringic acid cocrystals (TF–SYA cocrystal) had an enhanced inhibitory effect on different cancer cell lines (Fig. 23C)[179]. The improved solubility and dissolution rate of tegafur by the cocrystal were beneficial for generating higher drug concentrations near the tumor cells, thus impeding proliferation[179]. In addition, the permeability of tegafur was enhanced by the cocrystal, which allowed more drugs to penetrate the cytomembrane of tumor cells.

5-Fluorouracil (FU) is a classic anticancer drug for treating stomach, breast, lung and colorectal cancers. Therapeutic effect of 5-fluorouracil was limited by the poor permeability and first-pass hepatic metabolism of the drug. Therefore, massive doses are required to maintain the therapeutic window of FU, with the resulting risk of side effects of drug resistance. Recently, several 5-fluorouracil cocrystals with the enhanced anticancer bioactivity have been successfully prepared with coformers, such as L-phenylalanine[180], cinnamic acid[181], piperazine[182], gentisic acid[176], 3,4-dihydroxybenzoic acid[176], 4-aminopyridine[176] and hydroquinone[183]. For instance, the cocrystal of 5-fluorouracil–L-phenylalanine (FU–PHE) exhibited greater anticancer activity in comparison with the individual components (Fig. 24)[180]. The IC_{50} values of the FU–PHE cocrystal were significantly decreased in comparison with those of the pure FU and the FU–PHE physical mixture (Fig. 24C). The lowest IC_{50} value of cocrystals against HCT-116 cells was 2.56 μmol/L after 72 h of testing, which was approximately 4 times lower than that of pure 5-FU and the physical mixture. The

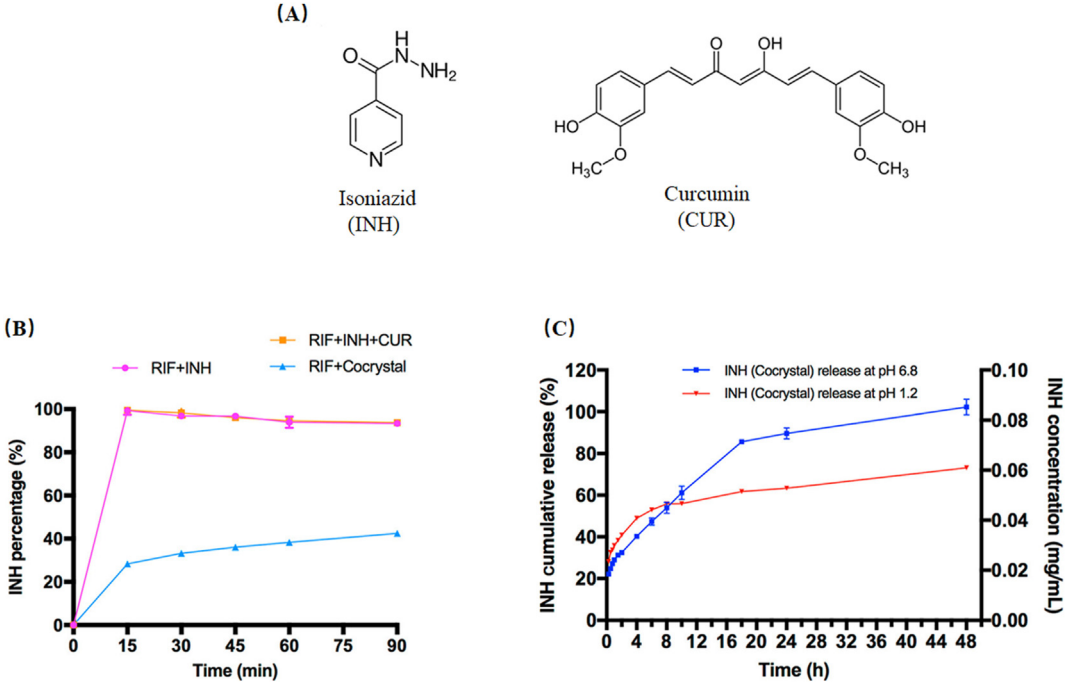

Figure 20 (A) Chemical structure of isoniazid and curcumin. (B) Dissolution profile of INH from different sample groups in pH 1.2 buffer solution. (C) Dissolution profile of INH from 2:1 INH–CUR cocrystals in the presence of RIF in pH 1.2 and 6.8 buffer solutions ($n = 3$). NOTE: RIF represents rifampicin. Adapted from the Ref. 173 with the permission. Copyright © 2020 American Chemical Society.

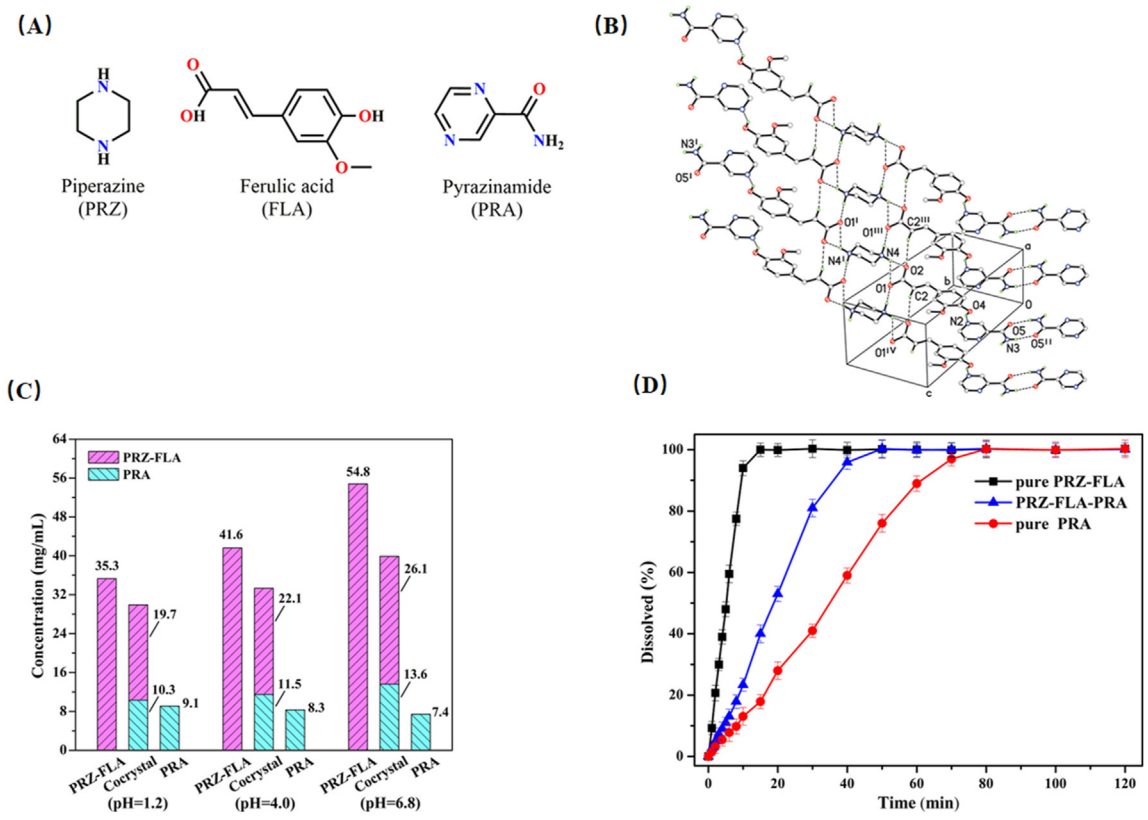

Figure 21 (A) The chemical structure of piperazine, ferulic acid, pyrazinamide. (B) The crystal structure of piperazine–ferulate–pyrazinamide cocrystal. (C) Solubility testing of piperazine ferulate salt (PRZ–FLA), cocrystal and pyrazinamide (PRA). (D) Intrinsic dissolution rate (IDR) testing of piperazine ferulate salt (PRZ–FLA), cocrystal and pyrazinamide (PRA) at pH 1.2. Adapted from the Ref. 165 with the permission. Copyright © 2020 American Chemical Society.

improved anticancer inhibition effect of FU–PHE contributes to the enhanced solubility, dissolution rate, permeability and increased tumor cell targeting of 5-FU in the presence of PHE, which is one of the essential amino acids for tumor cell growth.

Sulfamethazine (STH) is a sulfonamide drug that is a widely used antibacterial drug for treating humans and animals[184]. Recently, Pan and coworkers studied the antibacterial effect of the STH cocrystals (Fig. 25)[184]. *p*-Aminobenzoic acid (PABA) was selected as the coformer, forming a 1:1 cocrystal with STH by the slow evaporation crystallization method. Fig. 25B shows the antibacterial effect of the STH, PABA, physical mixture and sulfamethazine–*p*-aminobenzoic acid cocrystal (STH–PABA cocrystal) on *Escherichia coli,* a type of prokaryotic bacteria. The growth of *E. coli* was considerably inhibited in the group of the

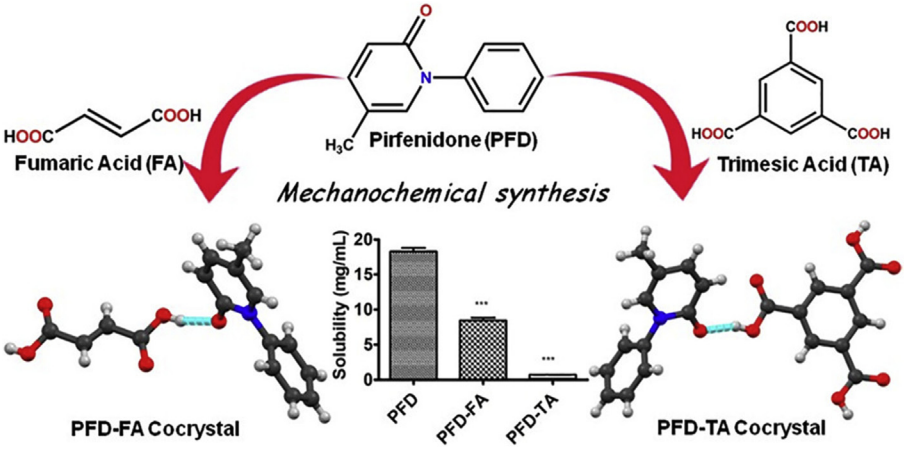

Figure 22 Chemical structure of pirfenidone (PFD), fumaric acid (FA) and trimesic acid (TA); hydrogen bonding between the PED–FA cocrystal and PFD–TA cocrystal; solubility results of the PFD, PFD–FA and PFD–TA cocrystals. Adapted from the Ref. 175 with the permission. Copyright © 2019 American Chemical Society.

Table 2 List of cocrystals with enhanced therapeutic effect.

Therapeutic category	API	Coformer	Ref.
Anticancer	Tegafur	Syringic acid	179
	5-Fluorouracil	L-Phenylalanine	180
		Cinnamic acid	181
		Piperazine	182
		Gentisic acid	176
		3,4-Dihydroxybenzoic acid	176
		4-Aminopyridine	176
		Hydroquinone	183
	Quinoxaline	3-Thiosemicarbano-butan-2-one-oxime	189
	Benzotriazole	*p*-Hydroxybenzoic acid	190
	Temozolomide	Oxalic acid	191
	Quercetin	Pyrazole	192
		Imidazolidinone	192
		Baclofen	192
	Metformin	Dichloroacetate	193
	Dabrafenib	Ethylenediamine hydrate	194
	Berberine Chloride	Myricetin	195
	Betulinic acid	Ascorbic acid	196
Antibacterial	Nitrofurantoin	Trimethoprim	197
	Ciprofloxacin	Carvacrol	198
		Thymol	198
	Sulfathiazole	Amantadine hydrochloride	177
	Enoxacin	Malonic acid	199
		Oxalic acid	199
		Fumaric acid	199
	Trimesic acid	Theophylline	200
		Caffeine	200
	Isopthalic acid	Caffeine	200
	Urotropine	Syringic acid	201
		trans-Cinnamic acid	201
		4-[4-(Trifluoromethyl) phenoxy] phenol	201
	Sulfamethazine	*p*-Aminobenzoic acid	184
	Sulfaguanidine	Thiobarbutaric acid	202
	Sulfadimidine	4-Aminosalicylic acid	203
	Genistein	4,4′-Bipyridine	204
	Benzotriazole	*p*-Hydroxybenzoic acid	190
	Caffeine	*O*-Formylphenoxyacetic acid monohydrate	205
		p-Formylphenoxypropionic acid	205
	Betulinic acid	Ascorbic acid	196
Hepatoprotective	Isoniazid	Syringic acid	206,207
		Quercetin	185,206
	Pyrazinamide	Quercetin	178
	Riluzole	Syringic acid	208
Arthritis	Diacerein	Isonicotinamide	209
		Nicotinamide	209
		Theophylline	209
	Aceclofenac	Lysine	210
	Hesperetin	Picolinic acid	186
		Nicotinamide	186
		Caffeine	186
	Chrysin	Cytosine	211
		Thiamine hydrochloride	211
Antihaemolytic	Hesperetin	Picolinic acid	186
		Nicotinamide	186
		Caffeine	186
	Chrysin	Cytosine	211
		Thiamine hydrochloride	211
	Quercetin	Nicotinamide	187
		Picolinic acid	187
Anti-diabetes	Glibenclamide	Hippuric acid	188
		Nicotinic acid	188
		Theophylline	188
		Succinic acid	188
	Nateglinide	Sucralose	212
	Gliclazide	Sebacic acid	213

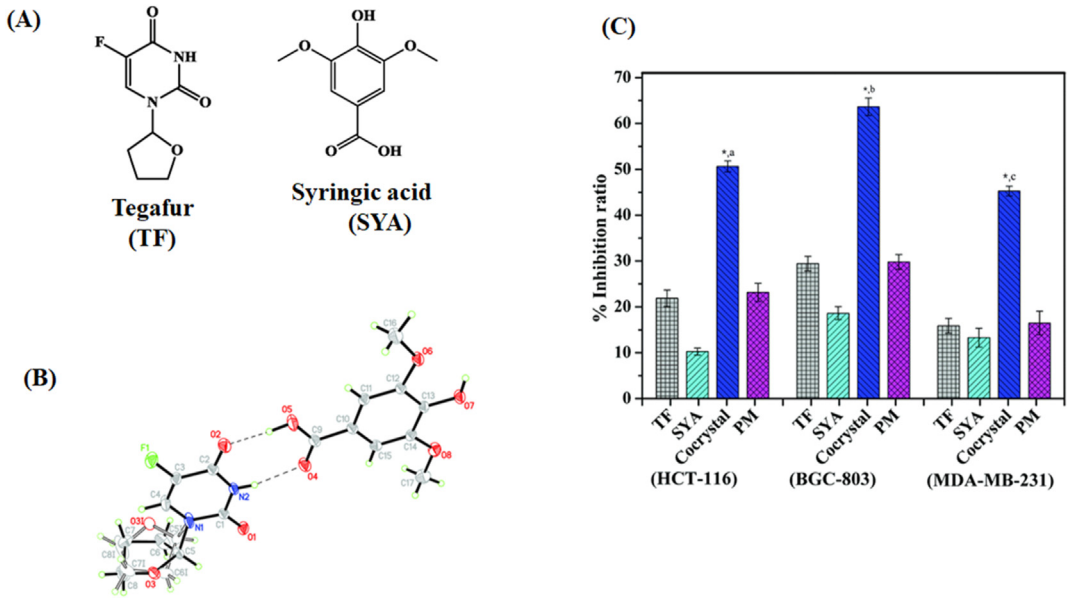

Figure 23 (A) Chemical structures of tegafur and syringic acid. (B) Crystal structure of tegafur–syringic acid cocrystal. (C) Cytotoxicity evaluation of individual materials, the cocrystal and physical mixture against the three tumor cell strains HCT-116 (human colon cancer), MDAMB-231 (breast cancer) and MGC-803 (human gastric carcinoma) by slforhodamine beta (SRB) assays. Note: a–c represent the CI values of the cocrystal of 0.79, 0.71, and 0.67 for HCT-116, MGC-803, and MDA-MB-231 tumor cell lines, respectively, $*P < 0.05$. Adapted from the Ref. 179 with the permission. Copyright © 2020 Royal Society of Chemistry.

cocrystal, with 2-fold higher antibacterial activity than that of pure STH at concentrations of 50 and 100 μg/mL. These results suggest that the enhanced antibacterial activity is due to the increased solubility of the cocrystals. As shown in Fig. 25C, the cell wall was intact with only several leaked cells in STH and PABA solutions after 12 h. However, the bacterial profile was significantly damaged in cocrystal solution, indicating that the leakage of cells would be enhanced by the STH–PABA cocrystal and thus drastically improve the antibacterial properties.

Long-term administration of high-dose isoniazid (INH) will cause server liver injury for patients[185]. The hepatotoxicity of INH is due to the generation of extremely high reactive oxygen species, which induce lipid peroxidation and eventually harm the cell membrane[185]. Liu et al.[185] studied *in vivo* hepatotoxicity testing of

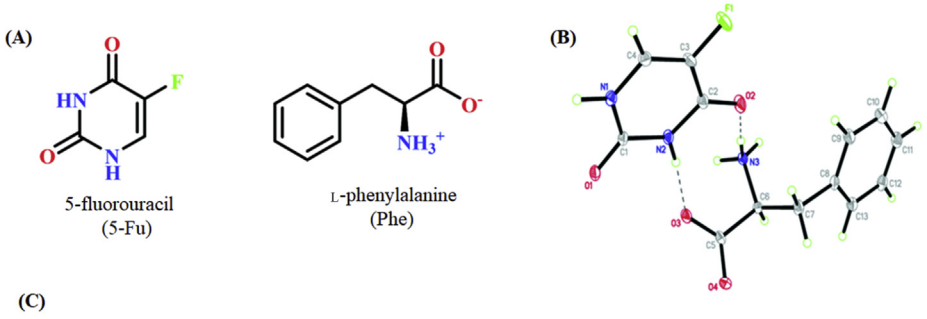

(C)

	HCT-116		MGC-803		MCF-7		A549	
Samples	48h	72h	48h	72h	48h	72h	48h	72h
Fu	18.82±2.08	10.83±0.29	19.41±0.62	8.62±0.82	20.39±2.61	15.27±1.13	24.72±2.62	13.60±1.09
Cocrystal	7.27±0.45	2.56±0.45	9.44±1.22	3.27±0.25	10.42±0.91	6.19±0.42	21.57±1.66	9.23±0.71
PM	16.41±1.45	9.02±0.37	17.48±0.41	6.56±0.86	19.65±1.07	13.94±1.74	24.13±0.47	11.73±0.94

Figure 24 (A) Chemical structures of 5-fluorouracil (Fu) and L-phenylalanine (Phe). (B) Crystal structure of 5-fluorouracil–L-phenylalanine cocrystal and (C) IC_{50} values (μmol/L) for the cell lines after 48 and 72 h exposure to the tested samples; note: HCT-116 (human colon cancer), MGC-803 (human gastric carcinoma), MCF-7 (human breast cancer), and A549 (human lung adenocarcinoma) were tested by SRB assay. Adapted from the Ref. 180 with the permission. Copyright © 2020 Royal Society of Chemistry.

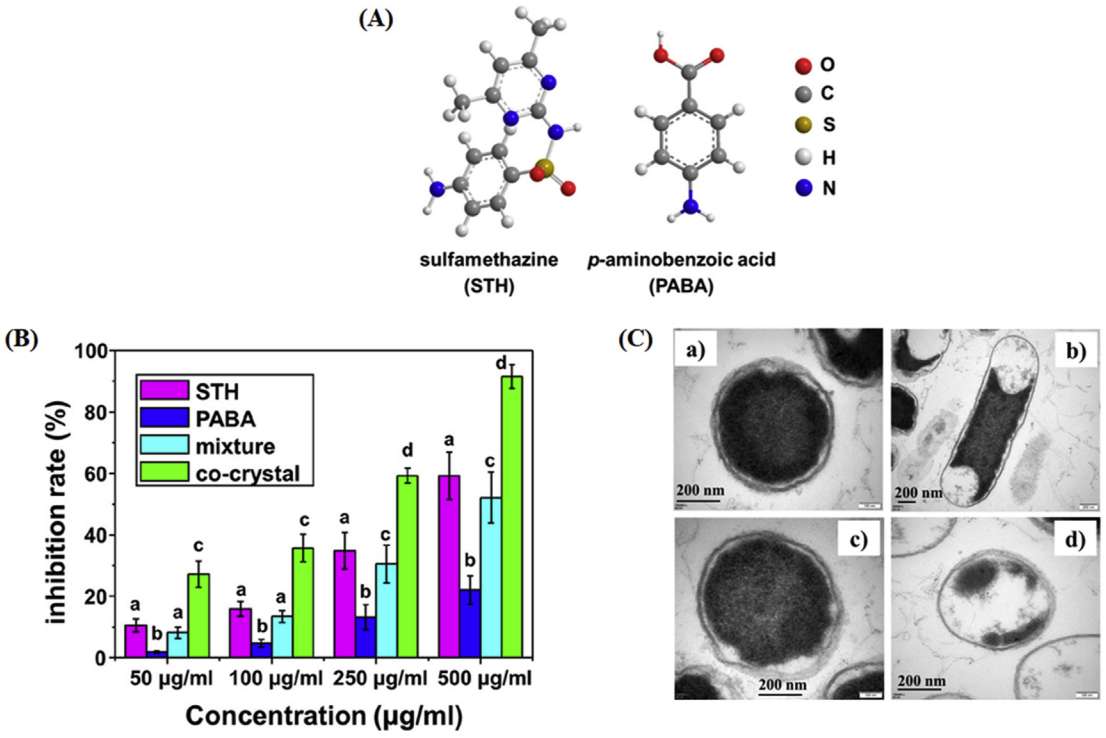

Figure 25 (A) Chemical structures of sulfamethazine (STH) and *p*-aminobenzoic acid (PABA). (B) Antibacterial effect of STH, PABA, physical mixture and STH–PABA cocrystal on *E. coli*. Different letters within the figure denote a significant difference ($P < 0.05$). (C) Transmission Electron Microscopy (TEM) images of *E. coli* before (a) and after treatment with 500 μg/mL STH (b), PABA (c), and cocrystals (d) for 12 h. Adapted from the Ref. 184 with the permission. Copyright © 2019 American Chemical Society.

untreated control, INH, a physical mixture of INH and quercetin (QCT) and isoniazid–quercetin cocrystal (INH–QCT cocrystal, Fig. 26). The total antioxidant states (TA), the level of aspartate aminotransferase (ASA) and alanine aminotransferase (ALA) of the four groups were measured after 3 days of treatment (Fig. 26B). For TA level testing, the cocrystal showed comparable value with the control group while the value of INH and the physical mixture group were lower in comparison with the control group, indicating that the cocrystal would improve the antioxidant effect of QCT to prevent the occurrence of hepatotoxicity during INH treatment. In addition, the levels of ASA and ALA were dramatically elevated after treatment with INH and the physical mixture because of the hepatotoxicity of INH. However, the values of ASA and ALA were similar to those in the control group in the cocrystal group. All results indicate that the cocrystallization of INH and QCT is effective in reducing INH-induced hepatotoxicity.

Chadha et al.[186] studied the antihemolytic effects of the cocrystals of nutraceutical hesperetin (HESP) with different

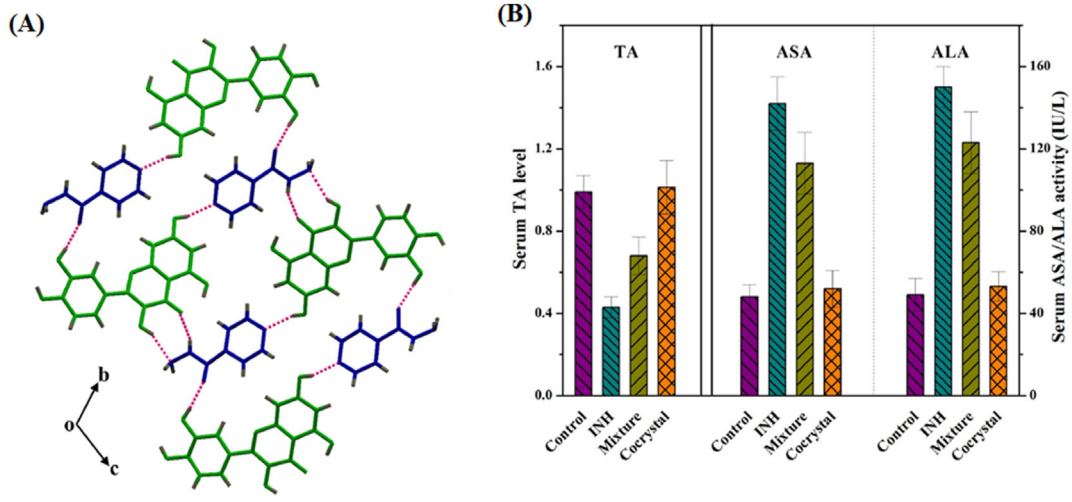

Figure 26 (A) Crystal structure of INH–QCT cocrystals and (B) protective effects of QCT against INH in cocrystals and mixtures detected by serum TA and liver enzyme levels in rats ($n = 6$). Adapted from the Ref. 185 with the permission. Copyright © 2020 Elsevier.

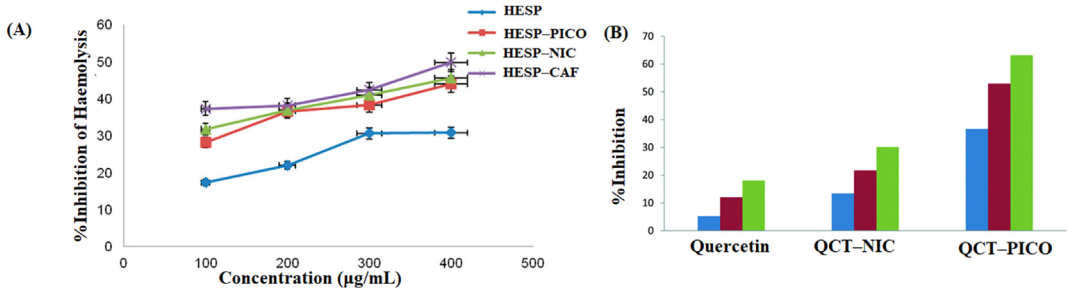

Figure 27 Percentage inhibition of hemolysis by (A) hesperetin and cocrystals. Adapted from the Ref. 186 with the permission. Copyright © 2017 American Chemical Society. (B) Different concetrations of quercetin and cocrystals: 50 μg/mL (blue color), 100 μg/mL (red color) and 150 μg/mL (green color). Adapted from the Ref. 187 with the permission. Copyright © 2016 Royal Society of Chemistry.

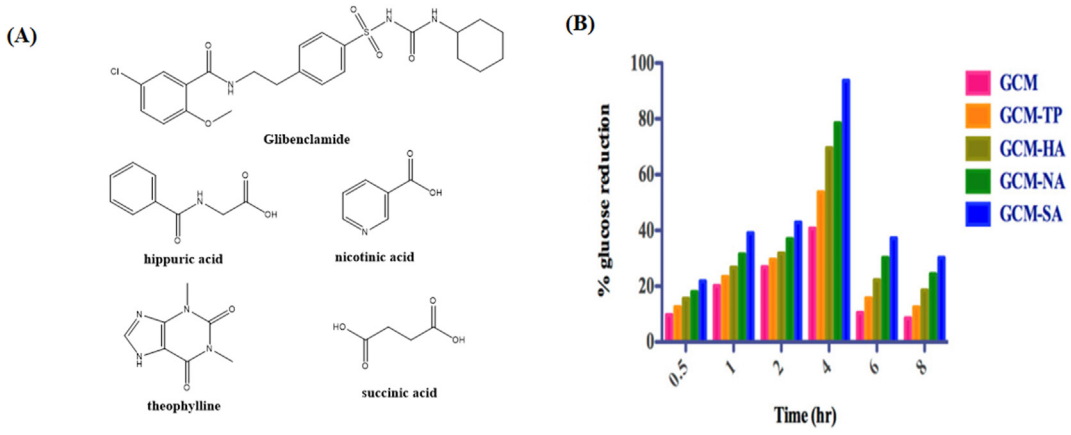

Figure 28 (A) The chemical structure of dlibenclamide, hippuric acid, nicotinic acid, theophylline and succinic acid. (B) Percentage of glucose reduction of GCM–HA, GCM–NA, GCM–TP, and GCM–SA in comparison to GCM. Adapted from the Ref. 188 with the permission. Copyright © 2018 American Chemical Society.

coformers, picolinic acid, nicotinamide, and caffeine. The cocrystals exhibited greater inhibition of hemolysis of rat RBSs than pure hesperetin (Fig. 27A). The inhibition effect of the samples is in the order hesperetin–caffeine cocrystal (HESP–CAF) > hesperetin–nicotinamide cocrystal (HESP–NIC) > hesperetin–picolinic acid cocrystal (HESP–PICO) > HESP. The maximum value of inhibition of hemolysis by HESP–CAF is 60%, followed by HESP–NIC (40%) and HESP–PICO (30%)[178]. Additionally, the cocrystals of quercetin–nicotinamide cocrystal (QCT–NIC) and quercetin–picolinic acid cocrystal (QCT–PICO) also displayed better antihemolytic activity than the pure substance (Fig. 27B)[187]. The percent inhibition of hemolysis in QCT–PICO and QCT–NIC was 3 and 2 times that of pure QCT, respectively[187]. The improved antihemolytic activity of cocrystals is linked to their higher solubilities and dissolution rates[187].

Glibenclamide (GCM) is a BCS class II drug for the treatment of type II (noninsulin-dependent) diabetes; it is a second-generation sulfonyl urea that has low solubility but high permeability. The plasma glucose levels of the rats in different systems were evaluated in protein-free plasma by enzymatic glucose oxidase peroxidase after 7 days of oral administration (Fig. 28)[188]. The maximum value of glucose reduction was up to 93.68% for glibenclamide–succinic acid cocrystal (GCM–SA), 78.46% for glibenclamide–nicotinic acid cocrystal (GCM–NA), 69.57% for glibenclamide–hippuric acid cocrystal (GCM–HA), 53.68% for glibenclamide–theophylline cocrystal (GCM–TP) and 40.68% for GCM[188].

4. Concluding remarks and future perspectives

In the past decade, cocrystal engineering has become a promising approach to improve the performance of drug substances by modifying their undesired physicochemical properties. Large numbers of pharmaceutical cocrystals have been reported, and some of them have been approved by the FDA or in the clinical trials[29]. Nevertheless there are still some considerable challenges for developing cocrystals into commercial drug products.

In designing a pharmaceutical cocrystal, it is critical to select a suitable coformer. However, the selection of coforms has still largely relied on trial and error, which is time consuming and labor-intensive. Recently, a variety of computer-assisted approaches have emerging as attractive tools to accelerate the screening process of cocrystals[214–218]. For example, the artificial neural network models are developed to predict cocrystal formation by analyzing a network of coformers extracted from the Cambridge Structural Database (CSD)[218].

An enhanced understanding of the structure-basis physicochemical properties is critical for the rational design of cocrystals with desired functions and performances. In addition, the compatibility between cocrystals and other excipients, pharmacokinetic

profiles, therapeutic efficacy and toxicity issues should be carefully taken into consideration in developing the formulation of cocrystal. Another hurdle for commercialization is the scale-up of high-purity pharmaceutical cocrystals. Continuous process is emerging as a new paradigm in high-throughput manufacture of pharmaceutical materials. The twin-screw extrusion integrated with process analytical tools for in-line process control has been attempted to produce high quality cocrystals[219,220].

In conclusions, this review provides detailed description and examples about preparation methods, physicochemical properties and various applications of cocrystals. The innovative technologies along with the comprehensive regulatory guidance will advance the translational development of pharmaceutical cocrystals for healthcare applications. More cocrystal-based drug products are believed to be commercially available for patients in the future.

Acknowledgments

The authors are grateful for the financial support to this work from the National Natural Science Foundation of China (Nos. 81872813), the Outstanding Youth Fund of Jiangsu Province of China (BK20190029), Natural Science Foundation of Jiangsu Province (BK 20200576, China), Fundamental Research Funds for the Central Universities (No. 2632020PY04) and the Program of State Key Laboratory of Natural Medicines-China Pharmaceutical University (No. SKLNMZZ202031).

Author contributions

Minshan Guo summarized the literatures and drafted the manuscript with the assistance of Xiaojie Sun and Jiahui Chen. Ting Cai conceived, supervised and edited the review. All of the authors have read and approved the final manuscript.

Conflicts of interest

The authors have no conflicts of interest to declare.

References

1. Cerreia Vioglio P, Chierotti MR, Gobetto R. Pharmaceutical aspects of salt and cocrystal forms of APIs and characterization challenges. *Adv Drug Deliv Rev* 2017;**117**:86−110.
2. Kalepu S, Nekkanti V. Insoluble drug delivery strategies: review of recent advances and business prospects. *Acta Pharm Sin B* 2015;**5**:442−53.
3. Schultheiss N, Newman A. Pharmaceutical cocrystals and their physicochemical properties. *Cryst Growth Des* 2009;**9**:2950−67.
4. Datta S, Grant DJW. Crystal structures of drugs: advances in determination, prediction and engineering. *Nat Rev Drug Discov* 2004;**3**:42−57.
5. Umeda Y, Fukami T, Furuishi T, Suzuki T, Tanjoh K, Tomono K. Characterization of multicomponent crystal formed between indomethacin and lidocaine. *Drug Dev Ind Pharm* 2009;**35**:843−51.
6. Karpinski PH. Polymorphism of active pharmaceutical ingredients. *Chem Eng Technol* 2006;**29**:233−7.
7. Khankari RK, Grant DJW. Pharmaceutical hydrates. *Thermochim Acta* 1995;**248**:61−79.
8. Healy AM, Worku ZA, Kumar D, Madi AM. Pharmaceutical solvates, hydrates and amorphous forms: a special emphasis on cocrystals. *Adv Drug Deliv Rev* 2017;**117**:25−46.
9. Remenar JF, Morissette SL, Peterson ML, Moulton B, Macphee JM, Guzmán HR, et al. Crystal engineering of novel cocrystals of a triazole drug with 1,4-dicarboxylic acids. *J Am Chem Soc* 2003;**125**:8456−7.
10. Duggirala NK, Perry ML, Almarsson Ö, Zaworotko MJ. Pharmaceutical cocrystals: along the path to improved medicines. *Chem Comm* 2015;**52**:640−55.
11. Yousef MAE, Vangala VR. Pharmaceutical co-crystals: molecules, crystals, formulations, medicines. *Cryst Growth Des* 2019;**19**:7420−38.
12. Karimijafari M, Padrela L, Walker G, Croker D. Creating cocrystals: a review of pharmaceutical cocrystal preparation routes and applications. *Cryst Growth Des* 2018;**18**:6370−87.
13. Novartis Pharmaceuticals Corporation. Drug trials snapshot: ENTRESTO. Approval date: July 7. 2015. Available from: https://www.fda.gov/drugs/drug-approvals-and-databases/drug-trials-snapshot-entresto.
14. Merck Sharpe & Dohme Corp. Drug trials snapshots: STEGLATRO. Approval date: December 19. 2017. Available from: https://www.fda.gov/drugs/drug-approvals-and-databases/drug-trials-snapshots-steglatro.
15. Videla S, Lahjou M, Vaqué A, Sust M, Encabo M, Soler L, et al. Single-dose pharmacokinetics of co-crystal of tramadol−celecoxib: results of a four-way randomized open-label phase I clinical trial in healthy subjects. *Br J Clin Pharmacol* 2017;**83**:2718−28.
16. Kimoto K, Yamamoto M, Karashima M, Hohokabe M, Takeda J, Yamamoto K, et al. Pharmaceutical cocrystal development of TAK-020 with enhanced oral absorption. *Crystals* 2020;**10**:211−29.
17. Huang S, Xu J, Peng Y, Guo M, Cai T. Facile tuning of the photoluminescence and dissolution properties of phloretin through cocrystallization. *Cryst Growth Des* 2019;**19**:6837−44.
18. Walsh RDB, Bradner MW, Fleischman AS, Morales LA, Zaworotko MJ. Crystal engineering of the composition of pharmaceutical phases. *Chem Comm* 2003;**9**:186−7.
19. Childs SL, Chyall LJ, Dunlap JT, Smolenskaya VN, Stahly BC, Stahly GP. Crystal engineering approach to forming cocrystals of amine hydrochlorides with organic acids. Molecular complexes of fluoxetine hydrochloride with benzoic, succinic, and fumaric acids. *J Am Chem Soc* 2006;**126**:13335−42.
20. Fleischman SG, Kuduva SS, Jennifer AM, Brian M, Walsh RDB, Rodríguez-Hornedo N, et al. Crystal engineering of the composition of pharmaceutical phases: multiple-component crystalline solids involving carbamazepine. *Cryst Growth Des* 2003;**3**:909−19.
21. Vishweshwar P, McMahon JA, Peterson ML, Hickey MB, Shattock TR, Zaworotko MJ. Crystal engineering of pharmaceutical co-crystals from polymorphic active pharmaceutical ingredients. *Chem Comm* 2005:4601−3.
22. Zaworotko MJ. Molecules to crystals, crystals to molecules ... and back again?. *Cryst Growth Des* 2007;**7**:4−9.
23. Shattock TR, Arora KK, Vishweshwar P, Zaworotko MJ. Hierarchy of supramolecular synthons: persistent carboxylic acid···pyridine hydrogen bonds in cocrystals that also contain a hydroxyl moiety. *Cryst Growth Des* 2008;**8**:4533−45.
24. Kale DP, Zode SS, Bansal AK. Challenges in translational development of pharmaceutical cocrystals. *J Pharm Sci* 2017;**106**:457−70.
25. Guide for industry. Regulatory classification of pharmaceutical co-crystals. U.S. Department of Health and Human Services Food and Drug Administration Center for Drug Evaluation and Research (CDER); December 2011. Availabe from: http://www.polycrystalline.it/filemanager/FDA%20guidance%20co%20crystals.pdf.
26. Guide for industry. Regulatory classification of pharmaceutical co-crystals. U.S. Department of Health and Human Services Food and Drug Administration Center for Drug Evaluation and Research (CDER); August 2016. Availabe from: https://www.fda.gov/media/99917/download.
27. Guide for industry. Regulatory classification of pharmaceutical co-crystals. U.S. Department of Health and Human Services Food and Drug Administration Center for rug Evaluation and Research (CDER); February 2018. Availabe from: https://www.fda.gov/media/81824/download.

28. EMA. Reflection paper on the use of cocrystals of active substances in medicinal products. 21 May 2015. Availabe from: https://www.ema.europa.eu/en/documents/scientific-guideline/reflection-paper-use-cocrystals-active-substances-medicinal-products_en.pdf.
29. Kavanagh ON, Croker DM, Walker GM, Zaworotko MJ. Pharmaceutical cocrystals: from serendipity to design to application. *Drug Discov Today* 2019;**24**:796−804.
30. Kuminek G, Cao F, Bahia de Oliveira da Rocha A, Gonçalves Cardoso S, Rodríguez-Hornedo N. Cocrystals to facilitate delivery of poorly soluble compounds beyond-rule-of-5. *Adv Drug Deliv Rev* 2016;**101**:143−66.
31. Chiarella RA, Davey RJ, Peterson ML. Making co-crystals the utility of ternary phase diagrams. *Cryst Growth Des* 2007;**7**:1223−6.
32. Blagden N, Berry DJ, Parkin A, Javed H, Ibrahim A, Gavan PT, et al. Current directions in co-crystal growth. *New J Chem* 2008;**32**:1659−72.
33. Weyna DR, Shattock T, Vishweshwar P, Zaworotko MJ. Synthesis and structural characterization of cocrystals and pharmaceutical cocrystals: mechanochemistry *vs* slow evaporation from solution. *Cryst Growth Des* 2009;**9**:1106−23.
34. Basavoju S, Boström D, Velaga SP. Pharmaceutical cocrystal and salts of norfloxacin. *Cryst Growth Des* 2006;**6**:2699−708.
35. Chow SF, Chen M, Shi L, Chow AHL, Sun CC. Simultaneously improving the mechanical properties, dissolution performance, and hygroscopicity of ibuprofen and flurbiprofen by cocrystallization with nicotinamide. *Pharm Res (N Y)* 2012;**29**:1854−65.
36. Modani S, Gunnam A, Yadav B, Nangia AK, Shastri NR. Generation and evaluation of pharmacologically relevant drug–drug cocrystal for gout therapy. *Cryst Growth Des* 2020;**20**:3577−83.
37. Nikam VJ, Patil SB. Pharmaceutical cocrystals of nebivolol hydrochloride with enhanced solubility. *J Cryst Growth* 2020;**534**:125488.
38. Rodrigues M, Baptista B, Lopes JA, Sarraguça MC. Pharmaceutical cocrystallization techniques. Advances and challenges. *Int J Pharm* 2018;**547**:404−20.
39. Wang IC, Lee MJ, Sim SJ, Kim WS, Chun NH, Choi GJ. Anti-solvent co-crystallization of carbamazepine and saccharin. *Int J Pharm* 2013;**450**:311−22.
40. Nishimaru M, Kudo S, Takiyama H. Cocrystal production method reducing deposition risk of undesired single component crystals in anti-solvent cocrystallization. *J Ind Eng Chem* 2016;**36**:40−3.
41. Lee MJ, Wang IC, Kim MJ, Kim P, Song KH, Chun NH, et al. Controlling the polymorphism of carbamazepine-saccharin cocrystals formed during antisolvent cocrystallization using kinetic parameters. *Korean J Chem Eng* 2015;**32**:1910−7.
42. Chun NH, Wang IC, Lee MJ, Jung YT, Lee S, Kim WS, et al. Characteristics of indomethacin−saccharin (IMC−SAC) co-crystals prepared by an anti-solvent crystallization process. *Eur J Pharm Biopharm* 2013;**85**:854−61.
43. Mullin JW. *Crystallization*. 4th ed. 2001. p. 536−75. Crystallization.
44. Yu ZQ, Chow PS, Tan RBH. Operating regions in cooling cocrystallization of caffeine and glutaric acid in acetonitrile. *Cryst Growth Des* 2010;**10**:2382−7.
45. Hickey MB, Peterson ML, Scoppettuolo LA, Morrisette SL, Vetter A, Guzmán H, et al. Performance comparison of a co-crystal of carbamazepine with marketed product. *Eur J Pharm Biopharm* 2007;**67**:112−9.
46. Sheikh AY, Rahim SA, Hammond RB, Roberts KJ. Scalable solution cocrystallization: case of carbamazepine-nicotinamide I. *CrystEngComm* 2009;**11**:501−9.
47. Leung DH, Lohani S, Ball RG, Canfield N, Wang Y, Rhodes T, et al. Two novel pharmaceutical cocrystals of a development compound—screening, scale-up, and characterization. *Cryst Growth Des* 2012;**12**:1254−62.
48. Zhao L, Raval V, Briggs NEB, Bhardwaj RM, McGlone T, Oswald IDH, et al. From discovery to scale-up: α-lipoic acid : nicotinamide co-crystals in a continuous oscillatory baffled crystalliser. *Cryst Eng Comm* 2014;**16**:5769−80.
49. Rodríguez-Hornedo N, Nehm SJ, Seefeldt KF, Pagán-Torres Y, Falkiewicz CJ. Reaction crystallization of pharmaceutical molecular complexes. *Mol Pharm* 2006;**3**:362−7.
50. Machado TC, Kuminek G, Cardoso SG, Rodríguez-Hornedo N. The role of pH and dose/solubility ratio on cocrystal dissolution, drug supersaturation and precipitation. *Eur J Pharm Sci* 2020;**152**:105422.
51. Cao F, Amidon GL, Rodriguez-Hornedo N, Amidon GE. Mechanistic analysis of cocrystal dissolution as a function of pH and micellar solubilization. *Mol Pharm* 2016;**13**:1030−46.
52. Maya P, Lipert Naír, Rodríguez-Hornedo. Cocrystal transition points: role of cocrystal solubility, drug solubility, and solubilizing agents. *Mol Pharm* 2015;**12**:3535−46.
53. Huang Y, Zhou L, Yang W, Li Y, Yin Q. Preparation of theophylline-benzoic acid cocrystal and on-line monitoring of cocrystallization process in solution by Raman spectroscopy. *Crystals* 2019;**9**:329−44.
54. Dai XL, Yao J, Wu C, Deng JH, Mo YH, Lu TB, et al. Solubility and permeability improvement of allopurinol by cocrystallization. *Cryst Growth Des* 2020;**20**:5160−8.
55. Ouiyangkul P, Tantishaiyakul V, Hirun N. Exploring potential coformers for oxyresveratrol using principal component analysis. *Int J Pharm* 2020;**587**:119630.
56. Yuan ZJ, Dai XL, Huang YL, Lu TB, Chen JM. Cocrystals of penciclovir with hydroxybenzoic acids: synthesis, crystal structures, and physicochemical evaluation. *Cryst Growth Des* 2020;**20**:4108−19.
57. Harfouche LC, Couvrat N, Sanselme M, Brandel C, Coquerel G. Discovery of new proxyphylline based chiral cocrystals: solid state landscape and dehydration mechanism. *Cryst Growth Des* 2020;**20**:3842−50.
58. Nagapudi K, Umanzor EY, Masui C. High-throughput screening and scale-up of cocrystals using resonant acoustic mixing. *Int J Pharm* 2017;**521**:337−45.
59. Michalchuk AAL, Hope KS, Kennedy SR, Blanco MV, Boldyreva EV, Pulham CR. Ball-free mechanochemistry: *in situ* real-time monitoring of pharmaceutical co-crystal formation by resonant acoustic mixing. *Chem Comm* 2018;**54**:4033−6.
60. am Ende DJ, Anderson SR, Salan JS. Development and scale-up of cocrystals using resonant acoustic mixing. *Org Process Res Dev* 2014;**18**:331−41.
61. Kaupp G. Solid-state molecular syntheses: complete reactions without auxiliaries based on the new solid-state mechanism. *Cryst Eng Comm* 2003;**5**:117−33.
62. Maheshwari C, Jayasankar A, Khan NA, Amidon GE, Rodríguez-Hornedo N. Factors that influence the spontaneous formation of pharmaceutical cocrystals by simply mixing solid reactants. *Cryst Eng Comm* 2009;**11**:493−500.
63. Macfhionnghaile P, Crowley CM, Mcardle P, Erxleben A. Spontaneous solid-state co-crystallization of caffeine and urea. *Cryst Growth Des* 2020;**20**:736−45.
64. Ervasti T, Aaltonen J, Ketolainen J. Theophylline−nicotinamide cocrystal formation in physical mixture during storage. *Int J Pharm* 2015;**486**:121−30.
65. Sarcevica I, Orola Ln, Nartowski KP, Khimyak YZ, Round AN, Fábián L. Mechanistic and kinetic insight into spontaneous cocrystallization of isoniazid and benzoic acid. *Mol Pharm* 2015;**12**:2981−92.
66. Nartowski KP, Khimyak YZ, Berry DJ. Tuning the spontaneous formation kinetics of caffeine: malonic acid co-crystals. *Cryst Eng Comm* 2016;**18**:2617−20.
67. Ji C, Hoffman MC, Mehta MA. Catalytic effect of solvent vapors on the spontaneous formation of caffeine−malonic acid cocrystal. *Cryst Growth Des* 2017;**17**:1456−9.
68. Sarcevica I, Orola L, Belyakov S, Veidis MV. Spontaneous cocrystal hydrate formation in the solid state: crystal structure aspects and kinetics. *New J Chem* 2013;**37**:2978−82.
69. Braga D, Grepioni F, Maini L, Prosperi S, Gobetto R, Chierotti MR. From unexpected reactions to a new family of ionic co-crystals: the

case of barbituric acid with alkali bromides and caesium iodide. *Chem Comm* 2010;**46**:7715−7.
70. Jayasankar A, Good DJ, Rodríguez-Hornedo N. Mechanisms by which moisture generates cocrystals. *Mol Pharm* 2007;**4**:360−72.
71. Huskić I, Christopherson JC, Užarević K, Friščić T. *In situ* monitoring of vapour-induced assembly of pharmaceutical cocrystals using a benchtop powder X-ray diffractometer. *Chem Comm* 2016; **52**:5120−3.
72. Chadwick K, Davey R, Cross W. How does grinding produce cocrystals? Insights from the case of benzophenone and diphenylamine. *Cryst Eng Comm* 2007;**9**:732−4.
73. Lien Nguyen K, Friščić T, Day GM, Gladden LF, Jones W. Terahertz time-domain spectroscopy and the quantitative monitoring of mechanochemical cocrystal formation. *Nat Mater* 2007;**6**:206−9.
74. Friščić T, Jones W. Recent advances in understanding the mechanism of cocrystal formation *via* grinding. *Cryst Growth Des* 2009;**9**: 1621−37.
75. Jayasankar A, Somwangthanaroj A, Shao ZJ, Rodríguez-Hornedo N. Cocrystal formation during cogrinding and storage is mediated by amorphous phase. *Pharm Res (N Y)* 2006;**23**:2381−92.
76. Rehder S, Klukkert M, Lobmann KA, Strachan CJ, Sakmann A, Gordon K, et al. Investigation of the formation process of two piracetam cocrystals during grinding. *Pharmaceutics* 2011;**3**: 706−22.
77. Karki S, Friščić T, Jones W. Control and interconversion of cocrystal stoichiometry in grinding: stepwise mechanism for the formation of a hydrogen-bonded cocrystal. *Cryst Eng Comm* 2009;**11**: 470−81.
78. Halasz I, Puškaric A, Kimber SAJ, Beldon PJ, Belenguer AM, Adams F, et al. Real-time *in situ* powder X-ray diffraction monitoring of mechanochemical synthesis of pharmaceutical cocrystals. *Angew Chem Int Ed* 2013;**52**:11538−41.
79. Fischer F, Scholz G, Benemann S, Rademann K, Emmerling F. Evaluation of the formation pathways of cocrystal polymorphs in liquid-assisted syntheses. *Cryst Eng Comm* 2014;**16**:8272−8.
80. Germann LS, Arhangelskis M, Etter M, Dinnebier RE, Friščić T. Challenging the ostwald rule of stages in mechanochemical cocrystallisation. *Chem Sci* 2020;**11**:10092−100.
81. Mukherjee A, Rogers RD, Myerson AS. Cocrystal formation by ionic liquid-assisted grinding: case study with cocrystals of caffeine. *CrystEngComm* 2018;**20**:3817−21.
82. Yan Y, Chen JM, Lu TB. Thermodynamics and preliminary pharmaceutical characterization of a melatonin−pimelic acid cocrystal prepared by a melt crystallization method. *Cryst Eng Comm* 2015;**17**: 612−20.
83. Liu X, Lu M, Guo Z, Huang L, Feng X, Wu C. Improving the chemical stability of amorphous solid dispersion with cocrystal technique by hot melt extrusion. *Pharm Res (N Y)* 2012;**29**: 806−17.
84. Seefeldt K, Miller J, Alvarez-Núñez F, Rodríguez-Hornedo N. Crystallization pathways and kinetics of carbamazepine−nicotinamide cocrystals from the amorphous state by *in situ* thermomicroscopy, spectroscopy, and calorimetry studies. *J Pharm Sci* 2007;**96**: 1147−58.
85. Guo C, Zhang Q, Zhu B, Zhang Z, Mei X. Drug−drug cocrystals provide significant improvements of drug properties in treatment with progesterone. *Cryst Growth Des* 2020;**20**:3053−63.
86. Duggirala NK, Smith AJ, Wojtas Ł, Shytle RD, Zaworotko MJ. Physical stability enhancement and pharmacokinetics of a lithium ionic cocrystal with glucose. *Cryst Growth Des* 2014;**14**:6135−42.
87. McKellar SC, Kennedy AR, McCloy NC, McBride E, Florence AJ. Formulation of liquid propofol as a cocrystalline solid. *Cryst Growth Des* 2014;**14**:2422−30.
88. Bacchi A, Capucci D, Giannetto M, Mattarozzi M, Pelagatti P, Rodriguez-Hormedo N, et al. Turning liquid propofol into solid (without freezing it): thermodynamic characterization of pharmaceutical cocrystals built with a liquid drug. *Cryst Growth Des* 2016; **16**:6547−55.
89. Liu F, Hooks DE, Li N, Mara NA, Swift JA. Mechanical properties of anhydrous and hydrated uric acid crystals. *Chem Mater* 2018;**30**: 3798−805.
90. Pudipeddi M, Serajuddin ATM. Trends in solubility of polymorphs. *J Pharm Sci* 2005;**94**:929−39.
91. Roy S, Quiñones R, Matzger AJ. Structural and physicochemical aspects of dasatinib hydrate and anhydrate phases. *Cryst Growth Des* 2012;**12**:2122−6.
92. Deng JH, Lu TB, Sun CC, Chen JM. Dapagliflozin-citric acid cocrystal showing better solid state properties than dapagliflozin. *Eur J Pharm Sci* 2017;**104**:255−61.
93. Huang S, Xue Q, Xu J, Ruan S, Cai T. Simultaneously improving the physicochemical properties, dissolution performance, and bioavailability of apigenin and daidzein by co-crystallization with theophylline. *J Pharm Sci* 2019;**108**:2982−93.
94. Syed TA, Gaikar VG, Mukherjee S. Stability of co-crystals of caffeine with gallic acid in presence of coformers. *J Food Process Eng* 2019;**42**:e13066.
95. Shinozaki T, Ono M, Higashi K, Moribe K. A novel drug–drug cocrystal of levofloxacin and metacetamol: reduced hygroscopicity and improved photostability of levofloxacin. *J Pharm Sci* 2019;**108**:2383−90.
96. Trask AV, Motherwell WDS, Jones W. Pharmaceutical cocrystallization: engineering a remedy for caffeine hydration. *Cryst Growth Des* 2005;**5**:1013−21.
97. Chen X, Li D, Luo C, Wang J, Deng Z, Zhang H. Cocrystals of zileuton with enhanced physical stability. *Cryst Eng Comm* 2018;**20**: 990−1000.
98. Nugraha YP, Uekusa H. Suppressed hydration in metoclopramide hydrochloride by salt cocrystallisation. *CrystEngComm* 2018;**20**: 2653−62.
99. Wang ZZ, Chen JM, Lu TB. Enhancing the hygroscopic stability of *S*-oxiracetam *via* pharmaceutical cocrystals. *Cryst Growth Des* 2012; **12**:4562−6.
100. Bofill L, Sande DD, Barbas R, Prohens R. New cocrystal of ubiquinol with high stability to oxidation. *Cryst Growth Des* 2020;**20**:5583−8.
101. Guo C, Zhang Q, Zhu B, Zhang Z, Bao J, Ding Q, et al. Pharmaceutical cocrystals of nicorandil with enhanced chemical stability and sustained release. *Cryst Growth Des* 2020;**20**: 6995−7005.
102. Ohashi Y, Yanagi K, Kurihara T, Sasada Y, Ohgo Y. Crystalline state reaction of cobaloxime complexes by X-ray exposure. 1. Direct observation of cobalt-carbon bond cleavage in [(*R*)-1-cyanoethyl][(*S*)-(−)-alpha-methylbenzylamine]bis(dimethylglyoximato)cobalt(III). *J Am Chem Soc* 1981;**103**:5805−12.
103. Ramirez MA, Borja NL. Epalrestat: an aldose reductase inhibitor for the treatment of diabetic neuropathy. *Pharmacotherapy* 2008;**28**: 646−55.
104. Putra OD, Umeda D, Nugraha YP, Nango K, Yonemochi E, Uekusa H. Simultaneous improvement of epalrestat photostability and solubility *via* cocrystallization: a case study. *Cryst Growth Des* 2018;**18**:373−9.
105. Steele JW, Faulds D, Goa KL. Epalrestat. A review of its pharmacology, and therapeutic potential in late-onset complications of diabetes mellitus. *Drugs Aging* 1993;**3**:532−55.
106. Wang JR, Yu Q, Dai W, Mei X. Drug−drug co-crystallization presents a new opportunity for the development of stable vitamins. *Chem Comm* 2016;**52**:3572−5.
107. Cha DS, Luo X, Ahmed J, Becirovic L, Cha RH, McIntyre RS. Brexpiprazole as an augmentation agent to antidepressants in treatment resistant major depressive disorder. *Expert Rev Neurother* 2019; **19**:777−83.
108. Arabiani M, Bal raju K, Bhunia S, Kranthi Teja P, Lodagekar A, Chavan R, et al. Brexpiprazole-catechol cocrystal: structure elucidation, excipient compatibility and stability. *CrystEngComm* 2019; **21**:6703−8.
109. Kristiina MH, Jarkko R. Prodrugs—an efficient way to breach delivery and targeting barriers. *Curr Top Med Chem* 2011;**11**: 2265−87.

110. Yuan LC, Dahl TC, Oliyai R. Effect of carbonate salts on the kinetics of acid-catalyzed dimerization of adefovir dipivoxil. *Pharm Res* 2000;**17**:1098−103 (N Y).
111. Lin RZ, Sun PJ, Tao Q, Yao J, Chen JM, Lu TB. Mechanism study on stability enhancement of adefovir dipivoxil by cocrystallization: degradation kinetics and structure-stability correlation. *Eur J Pharm Sci* 2016;**85**:141−8.
112. Gao Y, Gao J, Liu Z, Kan H, Zu H, Sun W, et al. Coformer selection based on degradation pathway of drugs: a case study of adefovir dipivoxil-saccharin and adefovir dipivoxil-nicotinamide cocrystals. *Int J Pharm* 2012;**438**:327−35.
113. Werbin H, Strom ET. Photochemistry of electron-transport quinones. I. model studies with 2-methyl-1,4-naphthoquinone (vitamin K3). *J Am Chem Soc* 1968;**90**:7296−301.
114. Zhu B, Wang JR, Zhang Q, Mei X. Improving dissolution and photostability of vitamin K3 *via* cocrystallization with naphthoic acids and sulfamerazine. *Cryst Growth Des* 2016;**16**:483−92.
115. Teraoka R, Fukami T, Furuishi T, Nagase H, Ueda H, Tode C, et al. Improving the solid-state photostability of furosemide by its cocrystal formation. *Chem Pharm Bull* 2019;**67**:940−4.
116. Yu Q, Yan Z, Bao J, Wang JR, Mei X. Taming photo-induced oxidation degradation of dihydropyridine drugs through cocrystallization. *Chem Comm* 2017;**53**:12266−9.
117. Fandiño OE, Reviglio L, Linck YG, Monti GA, Marcos Valdez MM, Faudone SN, et al. Novel cocrystals and eutectics of the antiprotozoal tinidazole: mechanochemical synthesis, cocrystallization, and characterization. *Cryst Growth Des* 2020;**20**:2930−42.
118. Seo M, Kwon J, Lee M, Kim J, Kim SJ, Yoon SH. Characterization of linagliptin−ferulic acid cocrystal with improved thermal and photostability. *Bull Korean Chem Soc* 2019;**40**:453−6.
119. Geng N, Chen JM, Li ZJ, Jiang L, Lu TB. Approach of cocrystallization to improve the solubility and photostability of tranilast. *Cryst Growth Des* 2013;**13**:3546−53.
120. Vangala VR, Chow PS, Tan RBH. Characterization, physicochemical and photo-stability of a co-crystal involving an antibiotic drug, nitrofurantoin, and 4-hydroxybenzoic acid. *CrystEngComm* 2011;**13**:759−62.
121. Mannava MKC, Gunnam A, Lodagekar A, Shastri NR, Nangia AK, Solomon KA. Enhanced solubility, permeability, and tabletability of nicorandil by salt and cocrystal formation. *Cryst Eng Comm* 2021;**23**:227−37.
122. Karki S, Friscic T, Fábián L, Laity P, Day G, Jones W. Improving mechanical properties of crystalline solids by cocrystal formation: new compressible forms of paracetamol. *Adv Mater* 2009;**21**:3905−9.
123. Chattoraj S, Shi L, Chen M, Velaga S, Sun C. Origin of deteriorated crystal plasticity and compaction properties of a 1:1 cocrystal between piroxicam and saccharin. *Cryst Growth Des* 2014;**14**:3864−74.
124. Yadav JP, Yadav RN, Uniyal P, Chen H, Jain S. Molecular interpretation of mechanical behavior in four basic crystal packing of isoniazid with homologous cocrystal formers. *Cryst Growth Des* 2020;**20**:832−44.
125. Singaraju A, Bahl D, Wang C, Swenson D, Sun C, Stevens L. Molecular interpretation of the compaction performance and mechanical properties of caffeine cocrystals: a polymorphic study. *Mol Pharm* 2020;**17**:21−31.
126. Joshi T, Singaraju A, Shah H, Morris K, Stevens L, Haware R. Structure-mechanics and compressibility profile study of flufenamic acid:nicotinamide cocrystal. *Cryst Growth Des* 2018;**18**:5853−65.
127. Bhatt JA, Bahl D, Morris K, Stevens LL, Haware RV. Structure-mechanics and improved tableting performance of the drug–drug cocrystal metformin:salicylic acid. *Eur J Pharm Biopharm* 2020;**153**:23−35.
128. Sun C, Grant DJW. Influence of crystal shape on the tableting performance of l-lysine monohydrochloride dihydrate. *J Pharm Sci* 2001;**90**:569−79.
129. Sun C, Hou H. Improving mechanical properties of caffeine and methyl gallate crystals by cocrystallization. *Cryst Growth Des* 2008;**8**:1575−9.
130. Bolla G, Nangia A. Pharmaceutical cocrystals: walking the talk. *Chem Comm* 2016;**52**:8342−60.
131. Mishra M, Mishra K, Narayan A, Reddy C, Vangala V. Structural basis for mechanical anisotropy in polymorphs of caffeine–glutaric acid cocrystal. *Cryst Growth Des* 2020;**20**:6306−15.
132. Roy P, Ghosh A. Mechanochemical cocrystallization to improve the physicochemical properties of chlorzoxazone. *Cryst Eng Comm* 2020;**22**:4611−20.
133. Paul S, Taylor LJ, Murphy B, Krzyzaniak J, Dawson N, Mullarney MP, Meenan P, Sun CC. Mechanism and kinetics of punch sticking of pharmaceuticals. *J Pharm Sci* 2017;**106**:151−8.
134. Wang C, Paul S, Sun D, Nilsson Lill S, Sun C. Mitigating punch sticking propensity of celecoxib by cocrystallization: an integrated computational and experimental approach. *Cryst Growth Des* 2020;**20**:4217−23.
135. Varughese PS, Mangalampalli K, Solonko K, Bond A, Ramamurty U, Desiraju G. Interaction anisotropy and shear instability of aspirin polymorphs established by nanoindentation. *Chem Sci* 2011;**2**:2236−42.
136. Lv S, Dudek DM, Cao Y, Balamurali MM, Gosline J, Li H. Designed biomaterials to mimic the mechanical properties of muscles. *Nature* 2010;**465**:69−73.
137. Hayashi S, Yamamoto Sy, Takeuchi D, Ie Y, Takagi K. Creating elastic organic crystals of π-conjugated molecules with bending mechanofluorochromism and flexible optical waveguide. *Angew Chem Int Ed* 2018;**57**:17002−8.
138. Bhattacharya B, Roy D, Dey S, Puthuvakkal A, Bhunia S, Mondal S, et al. Mechanical-bending-induced fluorescence enhancement in plastically flexible crystals of a GFP chromophore analogue. *Angew Chem Int Ed* 2020;**59**:19878−83.
139. Lai S, Temiño I, Cramer T, Del Pozo F, Fraboni B, Cosseddu P, et al. Morphology influence on the mechanical stress response in bendable organic field—effect transistors with solution—processed semiconductors. *Adv Electron Mater* 2017;**4**:1700271.
140. Ghosh S, Reddy CM. Elastic and bendable caffeine cocrystals: implications for the design of flexible organic materials. *Angew Chem Int Ed* 2012;**51**:10319−23.
141. Li S, Yan D. Tuning light-driven motion and bending in macroscale flexible molecular crystals based on a cocrystal approach. *ACS Appl Mater Interfaces* 2018;**10**:22703−10.
142. Wang JR, Li M, Yu Q, Zhang Z, Zhu B, Qin W, Mei X. Anisotropic elasticity and plasticity of an organic crystal. *Chem Comm* 2019;**55**:8532−5.
143. Nguyen HN, Ha PT, Nguyen AS, Nguyen DT, Do HD, Thi QN, et al. Curcumin as fluorescent probe for directly monitoring *in vitro* uptake of curcumin combined paclitaxel loaded PLA-TPGS nanoparticles. *Adv Nat Sci Nanosci Nanotechnol* 2016;**7**:025001.
144. Gu Y, Zhao Z, Su H, Zhang P, Liu J, Niu G, et al. Exploration of biocompatible AIEgens from natural resources. *Chem Sci* 2018;**9**:6497−502.
145. Yan D, Evans DG. Molecular crystalline materials with tunable luminescent properties: from polymorphs to multi-component solids. *Mater Horiz* 2013;**1**:46−57.
146. Yan D, Delori A, Lloyd GO, Friščić T, Day GM, Jones W, et al. A cocrystal strategy to tune the luminescent properties of stilbene-type organic solid-state materials. *Angew Chem Int Ed* 2011;**50**:12483−6.
147. Wuest JD. Co-crystals give light a tune-up. Nat Chem;4:74-75.
148. Frenette M, Cosa G, Friščić T. Characterisation of organic solid forms and real-time *in situ* monitoring of their transformations using solid-state fluorescence. *Cryst Eng Comm* 2013;**15**:5100−6.
149. Li M, Li Z, Zhang Q, Peng B, Zhu B, Wang JR, et al. Fine-tuning the colors of natural pigment emodin with superior stability through cocrystal engineering. *Cryst Growth Des* 2018;**18**:6123−32.
150. Sangtani E, Sahu SK, Thorat SH, Gawade RL, Jha KK, Munshi P, et al. Furosemide cocrystals with pyridines: an interesting case of color cocrystal polymorphism. *Cryst Growth Des* 2015;**15**:5858−72.

151. Childs SL, Kandi P, Lingireddy SR. Formulation of a danazol cocrystal with controlled supersaturation plays an essential role in improving bioavailability. *Mol Pharm* 2013;**10**:3112−27.
152. Huang Y, Zhang B, Gao Y, Zhang J, Shi L. Baicalein−nicotinamide cocrystal with enhanced solubility, dissolution, and oral bioavailability. *J Pharm Sci* 2014;**103**:2330−7.
153. Dai XL, Li S, Chen JM, Lu TB. Improving the membrane permeability of 5-fluorouracil *via* cocrystallization. *Cryst Growth Des* 2016;**16**:4430−8.
154. Zhu B, Zhang Q, Wang JR, Mei X. Cocrystals of baicalein with higher solubility and enhanced bioavailability. *Cryst Growth Des* 2017;**17**:1893−901.
155. Smith AJ, Kavuru P, Wojtas L, Zaworotko MJ, Shytle RD. Cocrystals of quercetin with improved solubility and oral bioavailability. *Mol Pharm* 2011;**8**:1867−76.
156. Martin F, Pop M, Kacso I, Grosu IG, Baldea I. Ketoconazole-*p*-aminobenzoic acid cocrystal: revival of an old drug by crystal engineering. *Mol Pharm* 2019;**17**:919−32.
157. Ma XQ, Zhuang C, Wang BC, Huang YF, Chen Q, Lin N. Cocrystal of apigenin with higher solubility, enhanced oral bioavailability, and anti-inflammatory effect. *Cryst Growth Des* 2019;**19**:5531−7.
158. Haneef J, Markad D, Chadha R. Interaction map driven cocrystallization of ambrisentan: structural and biopharmaceutical evaluation. *Cryst Growth Des* 2020;**20**:4612−20.
159. Wang C, Tong Q, Hou X, Hu S, Fang J, Sun CC. Enhancing bioavailability of dihydromyricetin through inhibiting precipitation of soluble cocrystals by a crystallization inhibitor. *Cryst Growth Des* 2016;**16**:5030−9.
160. Ullah M, Shah MR, Asad MHHB, Hasan SMF, Hussain I. Improved *in vitro* and *in vivo* performanceofcarbamazepine enabled by using a succinic acidcocrystal in a stable suspension formulation. *Pak J Pharm Sci* 2017;**30**:2139−45.
161. Alhalaweh A, Ali HRH, Velaga SP. Effects of polymer and surfactant on the dissolution and transformation profiles of cocrystals in aqueous media. *Cryst Growth Des* 2014;**14**:643−8.
162. Zadymova NM, Poteshnova MV. Microemulsions and microheterogeneous microemulsion-based polymeric matrices for transdermal delivery of lipophilic drug (felodipine). *Colloid Polym Sci* 2019;**297**:453−68.
163. Albus H, Neidhart B. Membrane-controlled reagent-delivery systems—a new approach for the continuous production of reagent and standard solutions. *Fresen J Anal Chem* 2001;**370**:893−8.
164. Ma L. Progress in osmotic pump drug delivery system. *J China Pharm University* 2014;**45**:726−30.
165. Yu XZ, Wang LY, Liu F, Li YT, Yan CW. A sustained-release dual-drug ternary salt cocrystal of piperazine ferulate with pyrazinamide: the synthesis, structure and Hirshfeld surface analysis. *Cryst Growth Des* 2020;**20**:2064−73.
166. Aitipamula S, Cadden J, Chow PS. Cocrystals of zonisamide: physicochemical characterization and sustained release solid forms. *CrystEngComm* 2018;**20**:2923−31.
167. Somphon W, Prasertsabw A, Jarussophon N. Novel cogrinding of donepezil with neurotransmitters and coumarins: characterization, physical properties and *in vitro* drug release study. *Mater Today; Proc* 2019;**17**:1887−97.
168. Chen J, Li S, Lu TB. Pharmaceutical cocrystals of ribavirin with reduced release rates. *Cryst Growth Des* 2014;**14**:6399−408.
169. Deng Y, Zhang Y, Huang Y, Zhang M, Lou B. Preparation, crystal structures, and oral bioavailability of two cocrystals of emodin with berberine chloride. *Cryst Growth Des* 2018;**18**:7481−8.
170. Zhou J, Li L, Zhang H, Xu J, Huang D, Gong N, et al. Crystal structures, dissolution and pharmacokinetic study on a novel phosphodiesterase-4 inhibitor chlorbipram cocrystals. *Int J Pharm* 2020;**576**:118984.
171. Yuan Y, Li D, Wang C, Chen S, Zhang H. Structural features of sulfamethizole and its cocrystals: beauty within. *Cryst Growth Des* 2019;**2019**:7185−92.
172. Suresh K, Minkov VS, Namila KK, Derevyannikova E, Losev E, Nangia A, et al. Novel synthons in sulfamethizole cocrystals: structure−property relations and solubility. *Cryst Growth Des* 2015;**15**:3498−510.
173. Xuan B, Wong SN, Zhang Y, Weng J, Tong HHY, Wang C, et al. Extended release of highly water soluble isoniazid attained through cocrystallization with curcumin. *Cryst Growth Des* 2020;**20**:1951−60.
174. Maheshwari C, André V, Reddy S, Roy L, Duarte T, Rodríguez-Hornedo N. Tailoring aqueous solubility of a highly soluble compound *via* cocrystallization: effect of coformer ionization, pHmax and solute−solvent interactions. *CrystEngComm* 2012;**14**:4801−11.
175. Kumari N, Bhattacharya B, Roy P, Michalchuk AAL, Ghosh A. Enhancing the pharmaceutical properties of pirfenidone by mechanochemical cocrystallization. *Cryst Growth Des* 2019;**19**:6482−92.
176. Gautam MK, Besan M, Pandit D, Mandal S, Chadha R. Cocrystal of 5-fuorouracil: characterization and evaluation of biopharmaceutical parameters. *AAPS PharmSciTech* 2019;**20**:149.
177. Wang LY, Bu FZ, Li YT, Wu ZY, Yan CW. A sulfathiazole−amantadine hydrochloride cocrystal: the first codrug simultaneously comprising antiviral and antibacterial components. *Cryst Growth Des* 2020;**20**:3236−46.
178. Liu F, Wang LY, Li YT, Wu ZY, Yan CW. Protective effects of quercetin against pyrazinamide induced hepatotoxicity *via* a cocrystallization strategy of Ccomplementary advantages. *Cryst Growth Des* 2018;**18**:3729−33.
179. Yu YM, Yu MC, Wang LY, Li YT, Wu ZY, Yan CW. A supramolecular adduct of tegafur and syringic acid: the first tegafur-nutraceutical cocrystal with perfected *in vitro* and *in vivo* characteristics as well as synergized anticancer activities. *New J Chem* 2020;**44**:15994−6005.
180. Wang LL, Wang LY, Yu YM, Li YT, Wu ZY, Yan CW. Cocrystallization of 5-fluorouracil and l-phenylalanine: the first zwitterionic cocrystal of 5-fluorouracil with amino acid exhibiting perfect *in vitro/vivo* pharmaceutical properties. *CrystEngComm* 2020;**22**:5010−21.
181. Jubeen F, Liaqat A, Amjad F, Sultan M, Iqbal SZ, Sajid I, et al. Synthesis of 5-fluorouracil cocrystals with novel organic acids as coformers and anticancer evaluation against HCT-116 colorectal cell lines. *Cryst Growth Des* 2020;**20**:2406−14.
182. Muresan-Pop M, Chereches G, Borodi G, Fischer-Fodor E, Simon S. Structural characterization of 5-fluorouracil & piperazine new solid forms and evaluation of their antitumor activity. *J Mol Struct* 2020;**1207**:127842.
183. Suresh Kumar S, Athimoolam S, Sridhar B. Structural, spectral, theoretical and anticancer studies on new co-crystal of the drug 5-fluorouracil. *J Mol Struct* 2018;**1173**:951−8.
184. Pan X, Zheng Y, Chen R, Qiu S, Chen Z, Rao W, et al. Co-crystal of sulfamethazine and *p*-aminobenzoic acid: structural establishment and enhanced antibacterial properties. *Cryst Growth Des* 2019;**19**:2455−60.
185. Liu F, Wang LY, Yu MC, Li YT, Wu ZY, Yan CW. A new cocrystal of isoniazid-quercetin with hepatoprotective effect: the design, structure, and *in vitro/in vivo* performance evaluation. *Eur J Pharm Sci* 2020;**144**:105216.
186. Chadha K, Karan M, Bhalla Y, Chadha R, Khullar S, Mandal S, et al. Cocrystals of hesperetin: structural, pharmacokinetic, and pharmacodynamic evaluation. *Cryst Growth Des* 2017;**17**:2386−405.
187. Vasisht K, Chadha K, Karan M, Bhalla Y, Jena AK, Chadha R. Enhancing biopharmaceutical parameters of bioflavonoid quercetin by cocrystallization. *CrystEngComm* 2016;**18**:1403−15.
188. Goyal P, Rani D, Chadha R. Crystal engineering: a remedy to tailor the biopharmaceutical aspects of glibenclamide. *Cryst Growth Des* 2017;**18**:105−18.
189. Saha R, Sengupta S, Dey SK, Steele IM, Bhattacharyya A, Biswas S, et al. A pharmaceutical cocrystal with potential anticancer activity. *RSC Adv* 2014;**4**:49070−8.

190. Sathya P, Vidyalaksmi Y, Pugazhendhi S, Gopalakrishnan R. Benzotriazole *p*-hydroxybenzoic acid: physicochemical and biological evaluation of an organic cocrystal. *Mater Res Innov* 2016;**21**:182−8.
191. Kusuma Kanakaraju K, Lavanya V, Nangia A. Temozolomide cocrystals exhibit drug sensitivity in glioblastoma cells. *Proc Nat Acad Sci India A* 2014;**84**:321−30.
192. Veverka M, Dubaj T, Gallovič J, Jorík V, Veverková E, Danihelová M, et al. Cocrystals of quercetin: synthesis, characterization, and screening of biological activity. *Monat Chem* 2015;**146**:99−109.
193. Du J, Quan L, Feng W, Zhang Y. Metformin and dichloroacetate cocrystals suppress the growth of triple-negative breast cancer. *Lat Am J Pharm* 2019;**38**:1754−62.
194. Rai S, Gunnamm A, Mannava C, Nangia A. Improving the dissolution rate of anticancer drug dabrafenib. *Cryst Growth Des* 2020;**20**: 1035−46.
195. Li P, Ramaiah T, Zhang M, Zhang Y, Huang Y, Lou B. Two cocrystals of berberine chloride with myricetin and dihydromyricetin: crystal structures, characterization, and antitumor activities. *Cryst Growth Des* 2020;**20**:157−66.
196. Nicolov M, Ghiulai RM, Voicu M, Mioc M, Duse AO, Roman R, et al. Cocrystal formation of betulinic acid and ascorbic acid: synthesis, physico-chemical assessment, antioxidant, and antiproliferative activity. *Front Chem* 2019;**7**:92.
197. Maity DK, Paul RK, Desiraju GR. Drug−drug binary solids of nitrofurantoin and trimethoprim: crystal engineering and pharmaceutical properties. *Mol Pharm* 2020;**17**:4435−42.
198. Shemchuk O, d'Agostino S, Fiore C, Sambri V, Zannoli S, Grepioni F, et al. Natural antimicrobials meet a synthetic antibiotic: carvacrol/thymol and ciprofloxacin cocrystals as a promising solid-state route to activity enhancement. *Cryst Growth Des* 2020;**20**:6796−803.
199. Liu L, Zou D, Zhang Y, Zhang Q, Feng Y, Guo Y, et al. Pharmaceutical salts/cocrystals of enoxacin with dicarboxylic acids: enhancing *in vitro* antibacterial activity of enoxacin by improving the solubility and permeability. *Eur J Pharm Biopharm* 2020;**154**:62−73.
200. Abosede OO, Gordon AT, Dembaremba TO, Lorentino CMA, Frota HF, Santos ALS, et al. Trimesic acid−theophylline and isopthalic acid−caffeine cocrystals: synthesis, characterization, solubility, molecular docking, and antimicrobial activity. *Cryst Growth Des* 2020;**20**:3510−22.
201. Tabassum N, Varras PC, Arshad F, Choudhary MI, Yousuf S. Biological activity tuning of antibacterial urotropine *via* cocrystallization: synthesis, biological activity evaluation and computational insight. *CrystEngComm* 2020;**22**:3439−50.
202. Abidi SSA, Azim Y, Khan SN, Khan AU. Sulfaguanidine cocrystals: synthesis, structural characterization and their antibacterial and hemolytic analysis. *J Pharm Biomed Anal* 2018;**149**:351−7.
203. Serrano DR, Persoons T, D'Arcy DM, Galiana C, Dea-Ayuela MA, Healy AM. Modelling and shadowgraph imaging of cocrystal dissolution and assessment of *in vitro* antimicrobial activity for sulfadimidine/4-aminosalicylic acid cocrystals. *Eur J Pharm Sci* 2016;**89**:125−36.
204. Zhang YN, Yin HM, Zhang Y, Zhang DJ, Su X, Kuang HX. Preparation of a 1:1 cocrystal of genistein with 4,4′-bipyridine. *J Cryst Growth* 2017;**458**:103−9.
205. Kumar GSS, Seethalakshmi PG, Bhuvanesh N, Kumaresan S. Cocrystals of caffeine with formylphenoxyaliphatic acids: syntheses, structural characterization, and biological activity. *J Mol Struct* 2013; **1034**:302−9.
206. Yadav B, Gunnam A, Thipparaboina R, Nangia AK, Shastri NR. Hepatoprotective cocrystals of isoniazid: synthesis, solid state characterization, and hepatotoxicity studies. *Cryst Growth Des* 2019;**19**: 5161−72.
207. Liu F, Jiang FB, Li YT, Liu RM, Wu ZY, Yan CW. Cocrystallization with syringic acid presents a new opportunity for effectively reducing the hepatotoxicity of isoniazid. *Drug Dev Ind Pharm* 2020;**46**: 988−95.
208. Yadav B, Balasubramanian S, Chavan RB, Thipparaboina R, Naidu VGM, Shastri NR. Hepatoprotective cocrystals and salts of riluzole: prediction, synthesis, solid state characterization, and evaluation. *Cryst Growth Des* 2018;**18**:1047−61.
209. Tomar S, Chakraborti S, Jindal A, Grewal MK, Chadha R. Cocrystals of diacerein: towards the development of improved biopharmaceutical parameters. *Int J Pharm* 2019;**574**:118942.
210. Sharma G, Saini MK, Thakur K, Kapil N, Garg NK, Raza K, et al. Aceclofenac cocrystal nanoliposomes for rheumatoid arthritis with better dermatokinetic attributes: a preclinical study. *Nanomedicine* 2017;**12**:615−38.
211. Chadha R, Bhalla Y, Nandan A, Chadha K, Karan M. Chrysin cocrystals: characterization and evaluation. *J Pharm Biomed Anal* 2017; **134**:361−71.
212. Arafa MF, El-Gizawy SA, Osman MA, El Maghraby GM. Co-crystallization for enhanced dissolution rate of nateglinide: *in vitro* and *in vivo* evaluation. *J Drug Deliv Sci Tec* 2017;**38**:9−17.
213. Chadha R, Rani D, Goyal P. Supramolecular cocrystals of gliclazide: synthesis, characterization and evaluation. *Pharm Res (N Y)* 2017;**34**: 552−63.
214. Salem A, Nagy S, Pál S, Széchenyi A. Reliability of the hansen solubility parameters as co-crystal formation prediction tool. *Int J Pharm* 2019;**558**:319−27.
215. Sun G, Jin Y, Li S, Yang Z, Shi B, Chang C, et al. Virtual coformer screening by crystal structure predictions: crucial role of crystallinity in pharmaceutical cocrystallization. *J Phys Chem Lett* 2020;**11**: 8832−8.
216. Du JJ, Stanton SA, Williams PA, Ong JA, Groundwater PW, Overgaard J, et al. Using electron density to predict synthon formation in a 4-hydroxybenzoic acid : 4,4′-bipyridine co-crystal. *Cryst Growth Des* 2018;**18**:1786−98.
217. Zheng L, Zhu B, Wu Z, Fang X, Hong M, Liu G, et al. Strategy for efficient discovery of cocrystals *via* a network-based recommendation model. *Cryst Growth Des* 2020;**20**:6820−30.
218. Devogelaer JJ, Meekes H, Tinnemans P, Vlieg E, de Gelder R. Cocrystal prediction by artificial neural networks. *Angew Chem Int Ed* 2020;**59**:21711−8.
219. Gajda M, Nartowski KP, Pluta J, Karolewicz B. Continuous, one-step synthesis of pharmaceutical cocrystals *via* hot melt extrusion from neat to matrix-assisted processing—sate of the art. *Int J Pharm* 2019; **558**:426−40.
220. Moradiya HG, Islam MT, Scoutaris N, Halsey SA, Chowdhry BZ, Douroumis D. Continuous manufacturing of high quality pharmaceutical cocrystals integrated with process analytical tools for in-line process control. *Cryst Growth Des* 2016;**16**:3425−34.